Relativistic Hartree-Fock model for axially deformed nuclei

Jing Geng (耿晶),[1] Jian Xiang (向剑),[1] Bao Yuan Sun (孙保元),[1] and Wen Hui Long (龙文辉)[1,*]

[1] *School of Nuclear Science and Technology, Lanzhou University, Lanzhou 730000, China*

Axially deformed relativistic Hartree-Fock (RHF) model with density-dependent meson-nucleon couplings is established in this work, in which the integrodifferential Dirac equations are solved by expanding the Dirac spinor on the spherical Dirac Woods-Saxon base. Using the RHF Lagrangians PKOi ($i = 1, 2, 3$), the reliability of the method has been illustrated by taking the light ^{20}Ne, midheavy ^{56}Fe, and heavy Pb isotopes as examples. As a preliminary application, the systematic study of ^{20}Ne shows that PKO1 and PKO3, which contain the π-pseudovector (π-PV) coupling, improve the description of the binding energy of ^{20}Ne, as compared to PKO2 and the selected RMF Lagrangian. Moreover, it is found that the tensor force components carried by the π-PV coupling can present substantial effects in determining the shape evolution of nucleus.

PACS numbers: 21.60.Jz, 24.10.Jv, 24.30.Cz, 23.40.-s

* longwh@lzu.edu.cn

I. INTRODUCTIONS

In past decades, worldwide developments of the radioactive-ion-beam (RIB) facilities and advanced detectors [1–5] have largely enriched the field of nuclear physics, which has been extended from the traditional stable nuclei to the ones far from the stability line in nuclear chart, namely exotic nuclei [6–10]. Meanwhile, lots of novel nuclear phenomena have been observed when approaching the drip lines, such as the quenching of traditional magic shells and the emergences of new ones [11–19], the dilute matter distributions—halo phenomena [20–22], etc. Such interesting novel phenomena not only largely promote the development of nuclear physics with plentiful new opportunities, but also challenge our understanding on nuclear systems from both theoretical and experimental sides.

On the other hand, it is well known that most nuclei in the nuclear chart are deformed, except a few of them which locate nearby magic numbers. In the early 1950s, many evidences, such as the relationship between the nuclear quadruple moments and shell structure [23–27] , the rotational-like spectra [28, 29], etc., indicated that nuclei can have shape away from spherical. It is worthwhile to mention that some consequences of nuclear deformation were even discussed by Bohr and Kalckar in 1937 [30]. Recently, intensive attentions were paid on the evolution of nuclear shape because of the notable progress of the laser spectroscopy at RIB facilities [31, 32]. Being coupled with the deformation effects, more and more novel nuclear phenomena were discovered during the exploration of the boundary of the nuclear chart, such as the island of inversion [33–36], shape coexistence [37–39], the superdeformed and hyperdeformed configurations [40, 41], etc. In fact, intensive efforts have been devoted to understanding these colorful phenomena, which are potentially related to the deformation.

As one of the typical representatives, the relativistic mean field (RMF) theory founded on the meson exchange diagram of nuclear force [42], also referred to as the covariant density functional theory (CDFT) in recent years, provides an efficient and predictive tool in exploring the structure properties of nuclei which spread over almost the whole nuclear chart [43–49]. With a renormalized relativistic mean field, i.e., the so-call σ-ω model [50], the RMF theory presents an appropriate saturation mechanism of nuclear matter. Afterwards, in order to solve the problem of large incompressibility, intensive attempts have been devoted to the modeling of nuclear in-medium effects [51], either via the nonlinear self-couplings of meson fields [52–54] or the density dependencies of the meson-nucleon coupling strengths [55–58], and the accuracy and model reliability in describing various nuclear phenomena are largely improved with the proposed effective nuclear interactions. With the covariant representation of strong scalar and vector potentials of the order of several hundred MeV, the RMF theory provides simple and efficient descriptions of nuclear structure properties, such as the natural interpretation of strong spin-orbit couplings [59, 60] and the origin of pseudospin symmetry [61, 62].

Extending to the nuclei with deformation away from the spherical symmetry, large efforts were devoted to solving the partial differential Dirac equations of the nucleon in the relativistic framework, for instance by expanding the Dirac spinors on the analytic harmonic oscillator (HO) [63–65] or numerical Dirac Woods-Saxon (DWS) [66, 67] bases. For the former, the Dirac spinor and the relativistic mean field that contains only the Hartree terms of the meson-nucleon couplings are expanded in terms of fermionic and bosonic harmonic oscillators, respectively, which works well in exploring the structure properties of the axially deformed nuclei [44]. However, when extrapolating to the regions far from stability, namely exotic nuclei, it met serious difficulties in providing appropriate asymptotic behaviors of the wave functions because of the limit of the HO potential, particularly for halo nuclei. Although such defects may be overcome by considering a large mount of oscillator

shells [68], it strongly increases the numerical cost that in fact violates the simplicity of the HO base. Another alterative recipe is to employ the local-scaling point transformation to modify the unphysical asymptotic properties, namely the transformed HO base [69–71]. With the fast development of computational technology, it becomes possible to expand numerically the wave functions on the complete set made of the solutions of the Dirac equation with a Dirac Woods-Saxon potential [72], namely the DWS base [66]. Compared to the HO potential, the Woods-Saxon potential [73] would decrease smoothly to zero at large distance, which is essential to provide appropriate asymptotic behaviors of the density distributions, particularly for the exotic nuclei. Practically, the extension of the RMF theory—relativistic continuum Hartree-Bogoliubov (RCHB) theory [74]—has achieved great successes in describing not only spherical exotic nuclei [47], but also the axially deformed ones with the help of the DWS base [75–77]. As one of the typical examples, a novel mechanism—the decoupling between the deformations of the core and the halo in ^{44}Mg—has been predicted by the axially deformed RCHB theory [75].

Notice that the Fock terms, the inseparable part of the meson exchange diagram of nuclear force, are dropped in the RMF theory for simplicity. Thus, due to the limitation of the Hartree approach, the important degrees of freedom associated with the π and ρ-tensor couplings cannot be taken into account by the RMF approach. In particular the important ingredient—the tensor force, that plays significant role in nuclear shell evolutions [78, 79], symmetry energy [80], and excitations [81–85]—is also missing in the RMF scheme. In the past more than ten years, comparable accuracy as the conventional RMF model in describing nuclear structure properties has been achieved by the density dependent relativistic Hartree-Fock(DDRHF) theory [67, 86] with the proposed relativistic Hartree-Fock (RHF) Lagrangians PKOi(i = 1,2,3) [78, 86] and PKA1 [87]. Meanwhile, with the inclusion of the Fock terms, significant improvements are also obtained on the self-consistent description of nuclear shell evolutions [78, 79, 88, 89], tensor force [80, 90, 91], spin and isospin excitations [92–96], effective masses [86], symmetry energy [97–99], new magicity [89, 100, 101], and novel phenomena [101–103]. Thus, it would be quite valuable to investigate the effects of the Fock terms, particularly the π- and ρ-tensor couplings, in describing structure properties of deformed nuclei.

In fact, there already exists some attempt to extend the RHF theory to describe the deformed nuclei. In 2011, the relativistic Hartree-Fock-Bogoliubov (RHFB) model for axially deformed nuclei was established by expanding the Dirac spinors and RHF mean field on the deformed fermionic and bosonic HO bases, respectively [104]. However, due to the numerical complexity induced by the Fock terms, the calculations are quite time consuming, especially for the rearrangement terms due to the density dependencies of meson-nucleon coupling strengths, and the application is limited only for light deformed nuclei. On the other hand, it is not quite expectable in exploring the light exotic nuclei due to the limits of the HO base. In this work, as inspired by the successes achieved by the DDRHF theory, the axially deformed relativistic Hartree-Fock model is developed by expanding the Dirac spinors on the numerical DWS base, and as a preliminary application the role played by the π-pseudovector coupling in nuclear shape evolution is clarified by taking ^{20}Ne as an example. Notice that the pairing correlations are still restricted in the BCS scheme in this work, which works well in describing the nuclei nearby the stability line while less reliable for the unstable ones, particularly in exploring the halo structure in exotic nuclei [105]. Moreover, for the nuclei with super/hyperdeformation, the validity of the expansion on the spherical DWS basis should be tested more carefully, which is not the focus of the current work.

The paper is organized as follows. In Sec. II, we give the general formalism of the axially deformed RHF model based on the DWS base. In Sec. III, the results and discussions are presented, including the space truncation, the convergence check, and the description of ^{20}Ne by PKOi, in which the role of π-pseudovector coupling is analyzed. At the end, a summary is given in Sec. IV.

II. GENERAL FORMALISM

In this section, we will briefly recall the general formalism of the relativistic Hartree-Fock (RHF) theory, and the RHF energy functional of an axially deformed nucleus with the spherical Dirac Woods-Saxon (DWS) base. To give a complete impression to the readers, some details related to the density-dependent meson-nucleon coupling strengths, the pairing correlations, the DWS potentials, etc., will be also introduced. Meanwhile, the numerical difficulties in prior RHF calculations of deformed nuclei will be stressed to provide the readers an overall understanding of the status.

A. RHF Energy Functional

Based on the meson-exchange diagram of nuclear force, the Lagrangian density for nuclear systems, namely the starting point of the theory, can be constructed by considering the degrees of freedom associated with the Dirac field—nucleon (ψ) and meson fields—the isoscalar ones, including the σ meson (σ) and ω meson (ω^μ), and the isovector ones including the ρ meson ($\vec{\rho}^\mu$) and π meson ($\vec{\pi}$), and the photon field (A^μ). Among the selected degrees of freedom, the isoscalar mesons are introduced to take the strong attractions and repulsions between nucleons into account, and the isovector ones for the isospin-related aspects of nuclear force, and the photon field for the electromagnetic interactions between protons [51]. Therefore, the Lagrangian density for

nuclear systems can be expressed as

$$\mathscr{L} = \mathscr{L}_M + \mathscr{L}_\sigma + \mathscr{L}_\omega + \mathscr{L}_\rho + \mathscr{L}_\pi + \mathscr{L}_A + \mathscr{L}_I, \quad (1)$$

where the Lagrangians of the free fields $\mathscr{L}_\phi$ ($\phi = \psi, \sigma, \omega^\mu, \vec{\rho}^\mu, \vec{\pi}$, and A^μ) read as

$$\mathscr{L}_M = \bar{\psi}\left(i\gamma^\mu\partial_\mu - M\right)\psi, \quad (2)$$

$$\mathscr{L}_\sigma = +\frac{1}{2}\partial^\mu\sigma\partial_\mu\sigma - \frac{1}{2}m_\sigma^2\sigma^2, \quad (3)$$

$$\mathscr{L}_\omega = -\frac{1}{4}\Omega^{\mu\nu}\Omega_{\mu\nu} + \frac{1}{2}m_\omega^2\omega_\mu\omega^\mu, \quad (4)$$

$$\mathscr{L}_\rho = -\frac{1}{4}\vec{R}_{\mu\nu}\cdot\vec{R}^{\mu\nu} + \frac{1}{2}m_\rho^2\vec{\rho}^\mu\cdot\vec{\rho}_\mu, \quad (5)$$

$$\mathscr{L}_\pi = +\frac{1}{2}\partial_\mu\vec{\pi}\cdot\partial^\mu\vec{\pi} - \frac{1}{2}m_\pi^2\vec{\pi}\cdot\vec{\pi}, \quad (6)$$

$$\mathscr{L}_A = -\frac{1}{4}F^{\mu\nu}F_{\mu\nu}, \quad (7)$$

with the field tensors $\Omega^{\mu\nu} \equiv \partial^\mu\omega^\nu - \partial^\nu\omega^\mu$, $\vec{R}^{\mu\nu} \equiv \partial^\mu\vec{\rho}^\nu - \partial^\nu\vec{\rho}^\mu$, and $F^{\mu\nu} \equiv \partial^\mu A^\nu - \partial^\nu A^\mu$. Considering the Lorentz scalar (σ-S), vector (ω-V, ρ-V, and A-V), tensor (ρ-T), and pseudovector (π-PV) couplings, the Lagrangian density $\mathscr{L}_I$ that describes the interaction between nucleon and mesons (photon) reads as

$$\mathscr{L}_I = \bar{\psi}\Big(-g_\sigma\sigma - g_\omega\gamma^\mu\omega_\mu - g_\rho\gamma^\mu\vec{\tau}\cdot\vec{\rho}_\mu - e\gamma^\mu\frac{1-\tau_3}{2}A_\mu + \frac{f_\rho}{2M}\sigma_{\mu\nu}\partial^\nu\vec{\rho}^\mu\cdot\vec{\tau} - \frac{f_\pi}{m_\pi}\gamma_5\gamma^\mu\partial_\mu\vec{\pi}\cdot\vec{\tau}\Big)\psi. \quad (8)$$

In the Lagrangian densities, M and m_ϕ are the masses of the nucleon and mesons, and g_ϕ ($\phi = \sigma, \omega^\mu, \vec{\rho}^\mu$) and $f_{\phi'}$ ($\phi' = \vec{\rho}^\mu, \vec{\pi}$) represent the coupling strengths of various meson-nucleon couplings. In this paper, we use the arrows to denote the isovector quantities and the bold types for space vectors.

Following the standard variational procedure, one can derive the Dirac equations for the nucleon, Klein-Gordon equations for mesons, and Proca equation for photon from the Lagrangian density $\mathscr{L}$ as

$$\left(-i\gamma_\mu\partial^\mu + M + \Sigma\right)\psi(x) = 0, \quad (9)$$

$$\left(\Box + m_\sigma^2\right)\sigma = -g_\sigma\bar{\psi}\psi, \quad (10)$$

$$\left(\Box + m_\omega^2\right)\omega^\mu = +g_\omega\bar{\psi}\gamma^\mu\psi, \quad (11)$$

$$\left(\Box + m_\rho^2\right)\vec{\rho}^\mu = +g_\rho\bar{\psi}\gamma^\mu\vec{\tau}\psi - \partial_\nu\frac{f_\rho}{2M}\bar{\psi}\sigma^{\nu\mu}\vec{\tau}\psi, \quad (12)$$

$$\left(\Box + m_\pi^2\right)\vec{\pi} = +\partial_\nu\frac{f_\pi}{m_\pi}\bar{\psi}\gamma^5\gamma^\nu\vec{\tau}\psi, \quad (13)$$

$$\partial_\nu F^{\nu\mu} = e\bar{\psi}\frac{1-\tau_3}{2}\gamma^\mu\psi, \quad (14)$$

where the square box $\Box \equiv \partial_\mu\partial^\mu$. In the Dirac equation (9), the self-energy Σ can be obtained following the variational principle.

From the Lagrangian density (1), one can also obtain the Hamiltonian via the Legendre transformation. After neglecting the time-component of the four-momentum carried by the mesons and photon, and substituting the relevant equations, the Hamiltonian can be derived as

$$H = T + \sum_\phi V_\phi, \quad (15)$$

where the kinetic energy (T) and potential energy (V_ϕ) terms read as

$$T = \int d\boldsymbol{x}\bar{\psi}(\boldsymbol{x})\left(-i\boldsymbol{\gamma}\cdot\boldsymbol{\nabla} + M\right)\psi(\boldsymbol{x}), \quad (16)$$

$$V_\phi = \frac{1}{2}\int d\boldsymbol{x}d\boldsymbol{x}'\bar{\psi}(\boldsymbol{x})\bar{\psi}(\boldsymbol{x}')\Gamma_\phi D_\phi\psi(\boldsymbol{x}')\psi(\boldsymbol{x}). \quad (17)$$

In the potential energy terms V_ϕ, ϕ represents various two-body interaction channels, namely the σ-scalar (σ-S), ω-vector (ω-V), ρ-vector (ρ-V), ρ-tensor (ρ-T), ρ-vector-tensor (ρ-VT), π-pseudo-vector (π-PV), and photon-vector (A-V) couplings. The interaction vertex $\Gamma_\phi(x, x')$ are of the following form:

$$\Gamma_{\sigma\text{-S}} \equiv -g_\sigma(x)g_\sigma(x'), \quad (18a)$$

$$\Gamma_{\omega\text{-V}} \equiv \left(g_\omega\gamma_\mu\right)_x\left(g_\omega\gamma^\mu\right)_{x'}, \quad (18b)$$

$$\Gamma_{\rho\text{-V}} \equiv \left(g_\rho\gamma_\mu\vec{\tau}\right)_x\cdot\left(g_\rho\gamma^\mu\vec{\tau}\right)_{x'}, \quad (18c)$$

$$\Gamma_{\rho\text{-T}} \equiv \frac{1}{4M^2}\left(f_\rho\sigma_{\nu k}\vec{\tau}\partial^k\right)_x\cdot\left(f_\rho\sigma^{\nu l}\vec{\tau}\partial_l\right)_{x'}, \quad (18d)$$

$$\Gamma_{\rho\text{-VT}} \equiv \frac{1}{2M}\left(f_\rho\sigma^{k\nu}\vec{\tau}\partial_k\right)_x\cdot\left(g_\rho\gamma_\nu\vec{\tau}\right)_{x'} + \left(g_\rho\gamma_\nu\vec{\tau}\right)_x\cdot\frac{1}{2M}\left(f_\rho\sigma^{k\nu}\vec{\tau}\partial_k\right)_{x'}, \quad (18e)$$

$$\Gamma_{\pi\text{-PV}} \equiv \frac{-1}{m_\pi^2}\left(f_\pi\vec{\tau}\gamma_5\gamma_\mu\partial^\mu\right)_x\cdot\left(f_\pi\vec{\tau}\gamma_5\gamma_\nu\partial^\nu\right)_{x'}, \quad (18f)$$

$$\Gamma_{A\text{-V}} \equiv \frac{e^2}{4}\left[\gamma_\mu\left(1-\tau_3\right)\right]_x\left[\gamma^\mu\left(1-\tau_3\right)\right]_{x'}. \quad (18g)$$

After neglecting the retardation effects, namely ignoring the time component of the four-momentum carried by the mesons and photon, the propagators $D_\phi(\boldsymbol{x}, \boldsymbol{x}')$ in the potential terms V_ϕ read as

$$D_\phi = \frac{1}{4\pi}\frac{e^{-m_\phi|\boldsymbol{x}-\boldsymbol{x}'|}}{|\boldsymbol{x}-\boldsymbol{x}'|}, \qquad D_A = \frac{1}{4\pi}\frac{1}{|\boldsymbol{x}-\boldsymbol{x}'|}. \quad (19)$$

To get the energy functional, we restrict ourselves on the level of the mean field approach. Such that the nucleon field operator ψ in the Hamiltonian (16) can be quantized as

$$\psi(x) = \sum_i \psi_i(\boldsymbol{x})e^{-i\varepsilon_i t}c_i, \quad (20)$$

where the annihilation operators c_i are defined by the positive energy solutions of the Dirac equation (9), ε_i is the single-particle energy ($\varepsilon_i > 0$), and $\psi_i(\boldsymbol{x})$ is the Dirac spinor of state i. It should be noticed that in quantizing the nucleon spinor ψ [i.e., in Eq. (20)], the contributions from negative states are neglected, namely the no-sea approximation, in consistency with the mean

field approach that is often utilized in studying the ground state properties of nuclei [43, 44, 47, 106]. With the no-sea approximation, the energy functional E can be deduced from the expectation of Hamiltonian with respect to the Hartree-Fock ground state $|\Phi_0\rangle$ as

$$E = \langle\Phi_0| H |\Phi_0\rangle = \langle\Phi_0| T |\Phi_0\rangle + \sum_\phi \langle\Phi_0| V_\phi |\Phi_0\rangle , \quad (21)$$

$$|\Phi_0\rangle = \prod_{i=1}^{A} c_i^\dagger |0\rangle , \quad (22)$$

where A is the mass number of the nucleus, and $|0\rangle$ is the vacuum state. In the two-body interaction part V_ϕ, the expectation leads to two types of contributions, i.e., the direct Hartree and exchange Fock terms. If one considers only the Hartree terms, it leads to the so-called relativistic mean field (RMF) theory. If both the Hartree and Fock terms are taken into account, it corresponds to the relativistic Hartree-Fock (RHF) theory.

With the obtained energy functional, the variational operation,

$$\delta\Big[E - \sum_i \varepsilon_i \int d\boldsymbol{x}\psi_i^\dagger(\boldsymbol{x})\psi_i(\boldsymbol{x})\Big] = 0, \quad (23)$$

leads to the integrodifferential Dirac equation as

$$\int d\boldsymbol{x}' h(\boldsymbol{x},\boldsymbol{x}')\psi_i(\boldsymbol{x}') = \varepsilon_i\psi_i(\boldsymbol{x}), \quad (24)$$

where ε_i is the single-particle energy of the state i, and the single-particle Hamiltonian h contains three parts, namely the kinetic terms $h^{\rm kin}$, and the mean potential terms including the local contributions h^D and the ones from the Fock terms h^E:

$$h^{\rm kin} = \left[\boldsymbol{\alpha}\cdot\boldsymbol{p} + \gamma^0 M\right]\delta(\boldsymbol{x}-\boldsymbol{x}'), \quad (25)$$

$$h^D = \left[\Sigma_T(\boldsymbol{x})\gamma_5 + \Sigma_0(\boldsymbol{x}) + \gamma^0\Sigma_S(\boldsymbol{x})\right]\delta(\boldsymbol{x}-\boldsymbol{x}'), \quad (26)$$

$$h^E = \begin{pmatrix} Y_G(\boldsymbol{x},\boldsymbol{x}') & Y_F(\boldsymbol{x},\boldsymbol{x}') \\ X_G(\boldsymbol{x},\boldsymbol{x}') & X_F(\boldsymbol{x},\boldsymbol{x}') \end{pmatrix}. \quad (27)$$

In the above expressions, h^D contains the local scalar self-energy Σ_S, the time-component of the vector one Σ_0 and the tensor one Σ_T, and h^E contains the nonlocal mean fields X_G, X_F, Y_G, and Y_F contributed by the Fock terms. In considering the density dependencies in the meson-nucleon coupling strengths, namely taking g_ϕ ($\phi = \sigma, \omega^\mu, \vec{\rho}^\mu$) and $f_{\phi'}$ ($\phi' = \vec{\rho}^\mu, \vec{\pi}$) as functions of nucleon density $\rho_b = \bar{\psi}\gamma^0\psi$, the variation (23) may lead to an additional contribution to the self-energy Σ_0, i.e., the rearrangement terms Σ_R [58, 67, 86, 87].

B. Numerical difficulties in RHF descriptions of axially deformed nuclei

In this work, we restrict ourselves with the axial symmetry, i.e., focusing on the axially deformed nuclei. Standing on the level of the mean field approach, the nucleons are considered as point-like particles moving in an axially symmetric mean field. Consistent with the axial symmetry and reflection symmetry with respect to the $z = 0$ plane, the complete set of good quantum numbers is denoted as $(\nu\pi m)$, where ν is the principle quantum number, π represents the parity, and m is the projection of total angular momentum on the symmetric z axis. In the following, for simplicity, we use the index i to denote the quantum number set $(\nu\pi, m \lessgtr 0)$. The Dirac spinor of the nucleon in Eq. (20) is therefore of the following form with cylinder coordinate (ϱ, z, φ):

$$\psi_{\nu\pi m}(\varrho,z,\varphi) = \frac{1}{\sqrt{2\pi}} \begin{pmatrix} f^+_{\nu\pi}(\varrho,z)e^{i(m-1/2)\varphi} \\ f^-_{\nu\pi}(\varrho,z)e^{i(m+1/2)\varphi} \\ ig^+_{\nu\pi}(\varrho,z)e^{i(m-1/2)\varphi} \\ ig^-_{\nu\pi}(\varrho,z)e^{i(m+1/2)\varphi} \end{pmatrix}. \quad (28)$$

In practice it is not quite straightforward to solve the integrodifferential equation (24), particularly for the axially deformed nuclei.

Within the RMF approach, the Dirac equation (24) is reduced as a partial differential equation for the axially deformed nuclei. It can be solved by expanding the Dirac spinor on the deformed oscillator base, in which the local mean fields were also calculated by expansion in a deformed harmonic oscillator base [65]. In Ref. [104], a similar attempt has been performed to solve the integrodifferential Dirac equation for axially deformed nuclei, and both local and nonlocal mean fields were calculated via the expansion on axially deformed oscillator bases. However, the calculations of the nonlocal mean fields are too time consuming, particularly in dealing with the rearrangement terms generated by the density dependence of the coupling strengths [104], which largely limits the extensive study in heavy nuclei.

In cylindrical coordinate space (ϱ, z, φ), the meson propagators D_ϕ can be decomposed as

$$D_\phi = \frac{1}{4\pi}\sum_{\mu=-\infty}^{\infty} e^{i\mu(\varphi-\varphi')}\int_0^\infty \frac{kdk}{a_\phi(k)} \times J_\mu(k\varrho)J_\mu(k\varrho')e^{-a_\phi(k)|z-z'|}, \quad (29)$$

where $a_\phi(k) = \left(k^2 + m_\phi^2\right)^{1/2}$. Similar decomposition can be obtained for the photon D_A if set $m_\phi = 0$ [107]. As an alterative choice, one can solve the Dirac equation (24) by expanding the Dirac spinor on some selected base, such as the oscillator base [65, 104]. Then, the RHF mean fields can be calculated directly in cylinder coordinate space with the obtained wave functions. In principle, such procedure shall be valid for the RHF calculation of the axially deformed nuclei. However, in the expansion (29), the exponential term $\exp\left[-a_\phi(k)|z-z'|\right]$ will induce some singularity, i.e., rather sharp peaks appear at $z = z'$. This brings additional algorithm difficulty for the integration over the z coordinate. Moreover, the

Bessel functions J_μ result in the oscillating and rather slowly decaying integral term in Eq. (29). Numerically, it makes the precise calculation of the integration over k rather difficult.

In contrast to the cylindrical space, the propagator in the spherical coordinate space (r, ϑ, φ) can be expressed as [106, 108]

$$D_\phi = \sum_{\lambda_y \mu_y} (-1)^{\mu_y} R^\phi_{\lambda_y \lambda_y}(r, r') Y_{\lambda_y \mu_y}(\mathbf{\Omega}) Y_{\lambda_y - \mu_y}(\mathbf{\Omega}'), \quad (30)$$

where $\mathbf{\Omega} = (\vartheta, \varphi)$, the index λ_y is used to denote the expansion terms of the Yukawa propagator, and $R_{\lambda_y \lambda_y}$ contains the modified Bessel functions I and K as

$$R^\phi_{\lambda_y \lambda_y} = \frac{1}{2\pi} \frac{1}{\sqrt{rr'}} I_{\lambda_y + 1/2}(m_\phi r_<) K_{\lambda_y + 1/2}(m_\phi r_>), \quad (31)$$

$$R^A_{\lambda_y \lambda_y} = \frac{1}{2\pi} \frac{1}{2\lambda_y + 1} \frac{r_<^{\lambda_y}}{r_>^{\lambda_y + 1}}. \quad (32)$$

Comparing the expressions in cylindrical and spherical geometries, it is clear that the integration in Eq. (29) corresponds to the infinity sum over λ_y in Eq. (30) for given μ_y. Apparently, it is not an easy task to overcome the oscillating integration over k in Eq. (29).

Due to the mentioned algorithm difficulties, in this work, we consider the expansion of the Dirac spinor in a spherical Dirac Woods-Saxon (DWS) base [66, 67]. Compared to the oscillator one, the DWS base owns the advantages in providing appropriate asymptotical behaviors of the wave functions. It is essential for the reliable descriptions of the exotic nuclei. On the other hand, it will be similar to deal with the energy functional (21) as the spherical case [106], and the cutoff of the DWS base in expanding the Dirac spinor (28) will automatically truncate the infinity sum over λ_y in the propagator's expansion (30), which avoids the divergence naturally.

C. RHF energy functional for axially deformed nuclei with the DWS base

Restricted with the spherical symmetry, the complete set of good quantum numbers contains the principle one n, the angular momentum j and its projection m, and the parity $\pi = (-1)^l$ (l is the orbital angular momentum). For convenience, the quantum number κ is often used to denote the angular momentum j and the parity π, i.e., $\kappa = j + 1/2$ for $j = l - 1/2$ and $\kappa = -(j + 1/2)$ for $j = l + 1/2$, and $\pi = (-1)^\kappa \mathrm{sign}(\kappa)$ [108]. The Dirac spinor in the DWS base is of the following form:

$$\psi_{am}(\boldsymbol{x}) = \frac{1}{r} \begin{pmatrix} G_a(r) \Omega_{\kappa m}(\vartheta, \varphi) \\ i F_a(r) \Omega_{-\kappa m}(\vartheta, \varphi) \end{pmatrix}, \quad (33)$$

where the index a represents the set of quantum numbers $(n\kappa) = (njl)$, and $\Omega_{\kappa m}$ (also referred as Ω^l_{jm}) is the spherical spinor [108]. Here, we use l_u and l_d to denote the orbital angular momenta of the upper and lower components of the Dirac spinor ψ_{am}, respectively, and $l_u + l_d = 2j$. Notice that if the quantity κ denotes (jl_u), $-\kappa$ corresponds to (jl_d). Considering both positive and negative energy states in the spherical DWS base, the expansion of the spinor (28) can be expressed as

$$\psi_{\nu\pi m}(\boldsymbol{x}) = \sum_a C_{a,i} \psi_{am}(\boldsymbol{x}) = \sum_\kappa \psi_{\nu\kappa m}(\boldsymbol{x}), \quad (34)$$

where the expansion coefficient $C_{a,i}$ [i represents $(\nu\pi m)$] is restricted as a real number, and $\psi_{\nu\kappa m}$ reads as

$$\psi_{\nu\kappa m} = \sum_n C_{n\kappa,i} \psi_{n\kappa m} = \frac{1}{r} \begin{pmatrix} \mathcal{G}_{i\kappa} \Omega_{\kappa m} \\ i \mathcal{F}_{i\kappa} \Omega_{-\kappa m} \end{pmatrix}, \quad (35)$$

with $\mathcal{G}_{i\kappa} = \sum_n C_{n\kappa,i} G_{n\kappa}$ and $\mathcal{F}_{i\kappa} = \sum_n C_{n\kappa,i} F_{n\kappa}$.

In the present work, we concentrate on the RHF Lagrangian PKOi ($i = 1, 2, 3$) [78, 86]. Notice that PKO2 contains the σ-S, ω-V, ρ-V, and A-V couplings, and in addition PKO1 and PKO3 take the π-PV coupling into account. Thus, the RHF energy functional can be expressed as

$$E = E^{\mathrm{kin}} + \sum_\phi \left(E^D_\phi + E^E_\phi \right), \quad (36)$$

where $E^{\mathrm{kin}} = \langle \Phi_0 | T | \Phi_0 \rangle$, and E^D_ϕ and E^E_ϕ are the Hartree and Fock terms of the two-body potential energies $E_\phi = \langle \Phi_0 | V_\phi | \Phi_0 \rangle$ with $\phi = \sigma$-S, ω-V, ρ-V, π-PV, and A-V.

With the expansion (34), the kinetic energy functional E^{kin} can be derived as

$$E^{\mathrm{kin}} = \sum_i v_i^2 \sum_\kappa \int dr \Big\{ \mathcal{F}_{i\kappa} \Big[\frac{d\mathcal{G}_{i\kappa}}{dr} + \frac{\kappa}{r} \mathcal{G}_{i\kappa} - M \mathcal{F}_{i\kappa} \Big] - \mathcal{G}_{i\kappa} \Big[\frac{d\mathcal{F}_{i\kappa}}{dr} - \frac{\kappa}{r} \mathcal{F}_{i\kappa} - M \mathcal{G}_{i\kappa} \Big] \Big\}, \quad (37)$$

where v_i^2 ($\in [0, 2]$) denotes the occupations of the orbit i.

For PKOi, only the local self-energies Σ_S and Σ_0 remain in h^D Eq. (26), and the relevant scalar and baryon densities, i.e., ρ_s and ρ_b, can be deduced as

$$\rho_s = \sum_i \bar{\psi}_i(\boldsymbol{x}) \psi_i(\boldsymbol{x}) = \sum_{\lambda_d}^{\mathrm{even}} \rho_s^{\lambda_d}(r) P_{\lambda_d}(\cos\vartheta), \quad (38a)$$

$$\rho_b = \sum_i \bar{\psi}_i(\boldsymbol{x}) \gamma^0 \psi_i(\boldsymbol{x}) = \sum_{\lambda_d}^{\mathrm{even}} \rho_b^{\lambda_d}(r) P_{\lambda_d}(\cos\vartheta), \quad (38b)$$

where P_{λ_d} is the Legendre polynomial, λ_d shall be even integer starting from 0 because of the parity conservation, and the cutoff of λ_d is determined naturally by the truncation of the DWS base in the expansion (34). The expansion term ρ^{λ_d} can be derived as

$$\rho^{\lambda_d}(r) = \sum_i v_i^2 \sum_{\kappa\kappa'} (-1)^{m + \frac{1}{2}} \mathscr{D}^{\lambda_d 0}_{\kappa m, \kappa' m} \times \Big[\frac{\mathcal{G}_{i\kappa}(r) \mathcal{G}_{i\kappa'}(r)}{2\pi r^2} \pm \frac{\mathcal{F}_{i\kappa}(r) \mathcal{F}_{i\kappa'}(r)}{2\pi r^2} \Big], \quad (39)$$

where $\pm$ in squared brackets corresponds to the baryonic and scalar densities, respectively, and for the symbol $\mathscr{D}$ see Eq. (A4) for details.

With the expansion of densities (38), the Hartree terms of the energy functional E_ϕ^D can be expressed as

$$E^D_{\sigma\text{-S}} = \frac{2\pi}{2}\sum_{\lambda_d}\int r^2 dr \Sigma^{\lambda_d}_{S,\sigma\text{-S}}(r)\rho_s^{\lambda_d}(r), \tag{40a}$$

$$E^D_{\omega\text{-V}} = \frac{2\pi}{2}\sum_{\lambda_d}\int r^2 dr \Sigma^{\lambda_d}_{0,\omega\text{-V}}(r)\rho_b^{\lambda_d}(r), \tag{40b}$$

where the expansion term of self-energies are given in Eq. (A9). For the other two vector couplings, i.e., the ρ-V and A-V couplings, the expressions can be obtained similarly as the ω-V ones, and the details can be found in Appendix A 2.

For the contributions from the Fock terms to the energy functional (21), namely E_ϕ^E, they can be expressed in a unified form as

$$E_\phi^E = \frac{1}{2}\int dr dr' \sum_i v_i^2 \sum_{\kappa_1\kappa_2} \begin{pmatrix} \mathcal{G}_{i\kappa_1} & \mathcal{F}_{i\kappa_1}\end{pmatrix}_r \times \begin{pmatrix} Y^{\kappa_1,\kappa_2;\phi}_{G,\pi m} & Y^{\kappa_1,\kappa_2;\phi}_{F,\pi m} \\ X^{\kappa_1,\kappa_2;\phi}_{G,\pi m} & X^{\kappa_1,\kappa_2;\phi}_{F,\pi m}\end{pmatrix}_{r,r'} \begin{pmatrix} \mathcal{G}_{i\kappa_2} \\ \mathcal{F}_{i\kappa_2}\end{pmatrix}_{r'}, \tag{41}$$

where ϕ represents the σ-S coupling, the time and space components of the vector (ω-V, ρ-V, and A-V) ones, and the π-PV one. Here, we introduce $\mathcal{R}$ to denote the nonlocal density terms, which appear in the nonlocal self-energies Y_G, Y_F, X_G, and X_F as source terms,

$$\mathcal{R}^{++}_{\kappa\kappa',\pi m}(r,r') = \sum_\nu v_i^2 \mathcal{G}_{\nu\pi m,\kappa}(r)\mathcal{G}_{\nu\pi m,\kappa'}(r'), \tag{42}$$

$$\mathcal{R}^{+-}_{\kappa\kappa',\pi m}(r,r') = \sum_\nu v_i^2 \mathcal{G}_{\nu\pi m,\kappa}(r)\mathcal{F}_{\nu\pi m,\kappa'}(r'), \tag{43}$$

$$\mathcal{R}^{-+}_{\kappa\kappa',\pi m}(r,r') = \sum_\nu v_i^2 \mathcal{F}_{\nu\pi m,\kappa}(r)\mathcal{G}_{\nu\pi m,\kappa'}(r'), \tag{44}$$

$$\mathcal{R}^{--}_{\kappa\kappa',\pi m}(r,r') = \sum_\nu v_i^2 \mathcal{F}_{\nu\pi m,\kappa}(r)\mathcal{F}_{\nu\pi m,\kappa'}(r'). \tag{45}$$

For the details of the nonlocal self-energies Y_G, Y_F, X_G, and X_F in Eq. (41), the readers are referred to Appendix A 3.

D. Density dependent meson-nucleon couplings

In the current RHF approach, namely the DDRHF theory, the nuclear in-medium effects are introduced phenomenologically by taking the coupling strengths as the functions of density ρ_b [86, 87], i.e.,

$$g_\phi(\rho_b) = g_\phi(\rho_0) f_\phi(\xi), \qquad \text{for } \phi = \sigma\text{-S}, \omega\text{-V}, \tag{46a}$$

$$g_{\phi'}(\rho_b) = g_{\phi'}(0) e^{-a_{\phi'}\xi}, \qquad \text{for } g_{\phi'} = g_\rho, f_\rho, f_\pi, \tag{46b}$$

where $\xi = \rho_b/\rho_0$, ρ_0 is the saturation density, and

$$f_\phi(\xi) = a_\phi \frac{1 + b_\phi(\xi + d_\phi)^2}{1 + c_\phi(\xi + d_\phi)^2}. \tag{46c}$$

The parameters a, b, c, d in the expressions (46) are determined with the parametrization referring to the properties of nuclear matter and the selected finite nuclei [78, 86, 87].

Under the axial symmetry, the coupling constant g_ϕ can be expressed in terms of the Legendre polynomial as

$$g_\phi(\rho_b) = \sum_{\lambda_p}^{\text{even}} g_\phi^{\lambda_p}(\rho_b) P_{\lambda_p}(\cos\vartheta), \tag{47}$$

where λ_p shall be even integer due to the parity conservation and its cutoff is decided by the convergence requirement. The expansion term $g_\phi^{\lambda_p}$ is calculated by

$$g_\phi^{\lambda_p}(\rho_b) = \int_{-1}^{1} d(\cos\vartheta) P_{\lambda_p}(\cos\vartheta) g_\phi(\rho_b). \tag{48}$$

Because of the density dependence in g_ϕ, one has to take the rearrangement term Σ_R into account to preserve the energy-momentum conservation [58]. The variation of the coupling constants g_ϕ can be expressed as

$$\delta g_\phi(\rho_b) = \sum_{a,i}\sum_{\lambda_p} P_{\lambda_p}(\cos\vartheta) \sum_{\lambda_d} \frac{\partial g_\phi^{\lambda_p}}{\partial \rho_b^{\lambda_d}} \frac{\partial \rho_b^{\lambda_d}}{\partial C_{a,i}} \delta C_{a,i}, \tag{49}$$

where the fraction term $\partial\rho_b^{\lambda_d}/\partial C_{a,i}$ can be deduced easily from the expression of $\rho_b^{\lambda_d}$ (39), and the term $\partial g_\phi^{\lambda_p}/\partial\rho_b^{\lambda_d}$ is derived as

$$\frac{\partial g_\phi^{\lambda_p}}{\partial \rho_b^{\lambda_d}} = \sum_L \frac{\hat{\lambda}_p \hat{\lambda}_d}{\sqrt{2}\hat{L}} \left(C^{L0}_{\lambda_p 0 \lambda_d 0}\right)^2 \int_{-1}^{1} dt P_L(t) \frac{\partial g_\phi}{\partial \rho_b}, \tag{50}$$

where $\partial g_\phi/\partial\rho_b$ is determined by the density-dependent form (46), and $\hat{L} = \sqrt{2L+1}$. Notice that both $g_\phi^{\lambda_p}$ and $\partial g_\phi^{\lambda_p}/\partial\rho_b^{\lambda_d}$ are calculated numerically, in which the integration is evaluated with the Gaussian algorithm. Due to the density dependencies in the coupling strengths, the rearrangement terms, which appear in the self-energy $\Sigma_0^{\lambda_d}$, can be simply expressed as

$$\Sigma_R^{\lambda_d} = \sum_\phi \left(\Sigma^{D,\lambda_d}_{R,\phi} + \Sigma^{E,\lambda_d}_{R,\phi}\right), \tag{51}$$

where the detailed contributions from the Hartree and Fock terms are given in Appendices A 2 and A 3, respectively.

E. Eigenvalue equations: Dirac equations with the spherical DWS base

Since the Dirac spinors (28) are expanded on the spherical DWS base, the total energy of an axially

deformed nucleus is expressed as a functional of the coefficient set $\{C_{a,i}\}$. The variation (23) is therefore performed with respect to $C_{a,i}$, which leads to a series of eigenvalue equations as

$$H^{\pi m}\widehat{C}_i = \varepsilon_i \widehat{C}_i. \tag{52}$$

Notice that the expansion of the Dirac spinor [see Eq. (34)] contains $N = (N_F + N_D) \times K_m$ terms, and N_F, N_D and K_m will be introduced in the following context. Therefore, $H^{\pi m} = \left(H^{\pi m}_{aa'}\right)$ is a $N \times N$ square matrix, and $\widehat{C}_i = \left(C_{a,i}\right)$ is a column matrix with N terms. The eigenvalue, i.e., the single-particle energy ε_i, can be determined by diagonalizing $H^{\pi m}$, as well as the eigenvector $\widehat{C}_i$.

Similar to the single-particle Hamiltonian in the integrodifferential Dirac equation (24), the matrix $H^{\pi m}$ in Eq. (52) consists of three parts, i.e., the kinetic $H^{\rm kin}$, local H^D, and nonlocal H^E terms,

$$H = H^{\rm kin} + H^D + H^E, \tag{53}$$

where the subscript (πm) is omitted. With the spherical DWS base, the kinetic term can be expressed as,

$$H^{\rm kin}_{aa'} = \int dr \Big\{ -G_a\Big[\frac{dF_{a'}}{dr} - \frac{\kappa}{r}F_{a'} - MG_{a'}\Big] + F_a\Big[\frac{dG_{a'}}{dr} + \frac{\kappa}{r}G_{a'} - MF_{a'}\Big]\Big\}, \tag{54}$$

where $a = (n\kappa)$ and $a' = (n'\kappa')$, and for $H^{\rm kin}_{aa'}$ it requires $\kappa = \kappa'$. For the local $H^D_{aa'}$ that contains the Hartree mean fields and rearrangement terms, it can be expressed as

$$H^D_{aa'} = \int dr \sum_{\lambda_d} (-1)^{m+1/2} \mathscr{D}^{\lambda_d 0}_{\kappa m,\kappa' m} \begin{pmatrix} G_a & F_a \end{pmatrix} \times \left[\gamma_0 \Sigma^{\lambda_d}_{S,\sigma\text{-S}} + \sum_{\phi'} \Sigma^{\lambda_d}_{0,\phi'} + \Sigma^{\lambda_d}_R\right] \begin{pmatrix} G_{a'} \\ F_{a'} \end{pmatrix}, \tag{55}$$

where ϕ' represents the vector channels, i.e., the ω-V, ρ-V, and A-V couplings. For the nonlocal term, it can be expressed with the non-local mean field Y_G, Y_F, X_G, and X_F in the energy functional (41),

$$H^E_{aa'} = \sum_{\phi} \int dr dr' \begin{pmatrix} G_a & F_a \end{pmatrix}_r \times \begin{pmatrix} Y^{\kappa\kappa',\phi}_{G,\pi m} & Y^{\kappa\kappa',\phi}_{F,\pi m} \\ X^{\kappa\kappa,\phi}_{G,\pi m} & X^{\kappa\kappa',\phi}_{F,\pi m} \end{pmatrix}_{(r,r')} \begin{pmatrix} G_{a'} \\ F_{a'} \end{pmatrix}_{r'}. \tag{56}$$

In this work, we focus on the RHF Lagrangians PKOi ($i = 1, 2, 3$) and ϕ represents the σ-S, ω-V, ρ-V, π-PV, and A-V couplings.

F. Pairing correlations: BCS method with Gogny force

For the open-shell nuclei, the pairing correlations play an important role in determining the properties of ground state, particularly for the nuclei close to the drip line [47, 74, 109–112]. For the deformed nuclei, the pairing correlation also palys an essential role in the shape evolution of nucleus since the single-particle structure will be largely changed with the shape evolution. In this work, the pairing correlations are considered with the BCS scheme.

For the even-even nuclei, the BCS ground state can be expressed as

$$|\text{BCS}\rangle = \prod_i^{m>0} \left(u_i + v_i c^\dagger_i c^\dagger_{\bar{i}}\right)|-\rangle, \tag{57}$$

where v_i^2 ($\in [0,1]$) represents the occupation probabilities, $u_i^2 + v_i^2 = 1$, and $\bar{i}$ denotes the time reversal partner of the state i. From the variation with respect to v_i,

$$\delta \langle \text{BCS}| \left(H - \lambda \widehat{N}\right)|\text{BCS}\rangle = 0, \tag{58}$$

the gap equations can be derived as

$$\Delta_i = -\frac{1}{2}\sum_{i'}^{m'>0} V^{pp}_{ii'} \frac{\Delta_{i'}}{\sqrt{(\varepsilon_{i'} - \lambda)^2 + \Delta^2_{i'}}}, \tag{59}$$

where $\widehat{N}$ is the particle number operator, the chemical potential λ is introduced for particle number conservation, Δ_i is the pairing gap of state i, and the pairing interaction matrix element can be written in following general form as

$$V^{pp}_{ii'} = \langle i\bar{i}|\, V^{pp}\, |i'\bar{i}'\rangle - \langle i\bar{i}|\, V^{pp}\, |\bar{i}'i'\rangle. \tag{60}$$

In order to provide a reliable description of the pairing effects, we adopt the Gogny force D1S [113] as the pairing force to take advantage of the finite range, i.e., the natural convergence with the configuration space in evaluating the pairing effects. It is essential for the exploration of the shape evolution of the nucleus, since the single-particle spectrum is largely changed with respect to the deformation. The Gogny-type pairing force reads as

$$V^{pp}(\boldsymbol{r}, \boldsymbol{r}') = \sum_{\chi=1,2} e^{(\boldsymbol{r}-\boldsymbol{r}')^2/\mu^2_\chi}\big(W_\chi + B_\chi P^\sigma - H_\chi P^\tau - M_\chi P^\sigma P^\tau\big), \tag{61}$$

with the parameter $\mu_\chi, W_\chi, B_\chi, H_\chi$ and M_χ ($\chi = 1, 2$) as the finite range part of the Gogny force, and P^σ and P^τ are the spin and isospin exchange operators, respectively. Consistently with the expansion of the propagator (30), the coordinate part of V^{pp} is also expanded in spherical coordinate (r, ϑ, φ),

$$V_\chi(|\boldsymbol{r} - \boldsymbol{r}'|) = e^{(\boldsymbol{r}-\boldsymbol{r}')^2/\mu^2_\chi} = 2\pi \sum_{\lambda=0}^{\infty} V_{\chi,\lambda}(r, r') \sum_\mu Y_{\lambda\mu}(\vartheta, \varphi) Y^*_{\lambda\mu}(\vartheta', \varphi'), \tag{62}$$

where the radial part reads as

$$V_{\chi,\lambda}(r,r') = e^{-(r^2+r'^2)/\mu_\chi^2}\sqrt{2\pi\frac{\mu_\chi^2}{2rr'}}I_{\lambda+1/2}\Big(\frac{2rr'}{\mu_\chi^2}\Big). \quad (63)$$

In order to abbreviate the expression, we rewrite the Gogny pairing force as

$$V(\boldsymbol{r},\boldsymbol{r}') = 2\pi\sum_{\chi=1,2}\big(A_\chi + D_\chi P^\sigma\big)\sum_{\lambda=0}^{\infty}V_{\chi,\lambda}(r,r') \times\sum_{\mu}Y_{\lambda\mu}(\vartheta,\varphi)Y^*_{\lambda\mu}(\vartheta',\varphi'), \quad (64)$$

with $A_\chi = W_\chi - H_\chi P^\tau$ and $D_\chi = B_\chi - M_\chi P^\tau$. For given orbits i and i' in an axially deformed nucleus, the pairing interaction matrix element $V^{pp}_{ii'}$ can be derived under the spherical DWS base as

$$V^{pp}_{ii'} = \int dr dr' \sum_{\kappa\kappa'}\begin{pmatrix}K^G_{i\kappa,i'\kappa'} & K^F_{i\kappa,i'\kappa'}\end{pmatrix}_r \times\begin{pmatrix}\bar{Y}^G_{\kappa\kappa'} & \bar{Y}^F_{\kappa\kappa'}\\ \bar{X}^G_{\kappa\kappa'} & \bar{X}^F_{\kappa\kappa'}\end{pmatrix}_{(r,r')}\begin{pmatrix}K^G_{i\kappa,i'\kappa'}\\ K^F_{i\kappa,i'\kappa'}\end{pmatrix}_{r'}, \quad (65)$$

where $K^G_{i\kappa,i'\kappa'}$ and $K^F_{i\kappa,i'\kappa'}$ read as

$$K^G_{i\kappa,i'\kappa'}(r) = \frac{\mathcal{G}_{i\kappa}\mathcal{G}_{i'\kappa'}}{2\pi r^2}, \quad K^F_{i\kappa,i'\kappa'}(r) = \frac{\mathcal{F}_{i\kappa}\mathcal{F}_{i'\kappa'}}{2\pi r^2}, \quad (66)$$

and the nonlocal parts $\bar{Y}^G$, $\bar{Y}^F$, $\bar{X}^G$, and $\bar{X}^F$ have the following form:

$$\bar{Y}^G_{\kappa\kappa'} = \frac{1}{2}\sum_{\chi,\lambda}V_{\chi,\lambda}(r,r')\Big[\big(A_\chi+D_\chi\big)\big(C^{\lambda 0}_{j\frac{1}{2}j'-\frac{1}{2}}\big)^2 - D_\chi\big(C^{\lambda 0}_{l_u 0 l'_u 0}\big)^2\Big], \quad (67)$$

$$\bar{Y}^F_{\kappa\kappa'} = \frac{1}{2}\sum_{\chi,\lambda}V_{\chi,\lambda}(r,r')\big(A_\chi+D_\chi\big)\big(C^{\lambda 0}_{j\frac{1}{2}j'-\frac{1}{2}}\big)^2, \quad (68)$$

$$\bar{X}^G_{\kappa\kappa'} = \frac{1}{2}\sum_{\chi,\lambda}V_{\chi,\lambda}(r,r')\big(A_\chi+D_\chi\big)\big(C^{\lambda 0}_{j\frac{1}{2}j'-\frac{1}{2}}\big)^2, \quad (69)$$

$$\bar{X}^F_{\kappa\kappa'} = \frac{1}{2}\sum_{\chi,\lambda}V_{\chi,\lambda}(r,r')\Big[\big(A_\chi+D_\chi\big)\big(C^{\lambda 0}_{j\frac{1}{2}j'-\frac{1}{2}}\big)^2 - D_\chi\big(C^{\lambda 0}_{l_d 0 l'_d 0}\big)^2\Big]. \quad (70)$$

In the above expressions, the sum over λ shall fulfill $\lambda + l_u + l'_u$ to be even. Notice that in deriving $V^{pp}_{ii'}$, the L-S coupling scheme is used [74] and for simplicity we only consider the contribution of the main component $J = 0$ ($\boldsymbol{J} = \boldsymbol{L} + \boldsymbol{S}$).

G. Dirac Woods-Saxon potentials and deformation parameters

In calculating the nuclear structure under the CDFT, the self-consistent iteration starts in general from an initial potential. In this work, we take the local Dirac Woods-Saxon potentials [72] as the initial ones, which are also used in determining the spherical DWS base. The only difference is that in the initial DWS potential we need to consider the effects of deformation, i.e., to choose appropriate initial deformation parameters β_0. With the underlying iteration, the calculation will converge to a local minimum of the energy functional nearby β_0.

In the Dirac equation, the local self-energies consist of the vector and scalar terms, i.e., $\Sigma_0 + \gamma^0\Sigma_S$, which are also referred to as $\Sigma_\pm = \Sigma_0 \pm \Sigma_S$ for convenience. As an initial one, the local self-energy Σ_T and the nonlocal ones in Dirac equation (24) are set to be zero, and the Woods-Saxon type local $\Sigma_\pm$ can be expressed as follows:

$$\Sigma^{\tau_3}_+(r) = +V_0\frac{1-a_0(N-Z)\tau_3/A}{1+\exp\big[(r-R^{\tau_3}_+)/a^{\tau_3}_+\big]} + V_c^{\tau_3}, \quad (71a)$$

$$\Sigma^{\tau_3}_-(r) = -V_0\frac{a_v^{\tau_3}\,[1-a_0(N-Z)\tau_3/A]}{1+\exp\big[(r-R^{\tau_3}_-)/a^{\tau_3}_-\big]} + V_c^{\tau_3}, \quad (71b)$$

where the isospin projection operator τ_3 is defined with the convention that $\tau_3|n\rangle = |n\rangle$ and $\tau_3|p\rangle = -|p\rangle$, and $R^{\tau_3}_\pm = r^{\tau_3}_{0,\pm}A^{1/3}$ represent the empirical radius of neutron or proton for the nucleus with mass number A, and $V_c^{\tau_3}$ represents the Coulomb potential between protons ($\tau_3 = -1$). The parameters in the Dirac Woods-Saxon potential, being used in this work to provide the spherical DWS base and initial potential, are given in Table I.

TABLE I. Parameters of the Dirac Woods-Saxon potential, and $V_0 = -71.28$ MeV and $a_0 = 0.4616$ [72]. Except the dimensionless a_v, the other parameters are in fm.

	a_v	$r_{0,+}$	$r_{0,-}$	a_+	a_-
Neutron	11.1175	1.2334	1.1443	0.615	0.6476
Proton	8.9698	1.2496	1.1400	0.6124	0.6469

In the Dirac Woods-Saxon potentials (71), the Coulomb potential between protons is evaluated by assuming the charge distributed uniformly,

$$V_c = \alpha Z\Big(\frac{3}{2R_c} - \frac{r^2}{2R_c^3}\Big), \quad \text{when } r < R_c, \quad (72a)$$

$$V_c = \alpha Z\frac{1}{r}, \quad \text{when } r \geqslant R_c, \quad (72b)$$

where $R_c = R^{\tau_3=-1}_+$, and α is the fine-structure constant that represents the coupling strength of Coulomb interaction.

Different from determining the spherical DWS base, one has to take the deformation effects into account in the initial DWS potentials (71). If restricted with the spherical symmetry, one can divide a nucleus into spherical shells with equal density at various radial distances. Extending to an axially deformed nucleus, the surface with equal density becomes an ellipsoidal one,

which can be described as

$$R(\vartheta,\varphi) = R_0\Big[1+\sum_{\lambda\mu}\alpha_{\lambda\mu}Y_{\lambda\mu}(\vartheta,\varphi)\Big], \tag{73}$$

where R_0 corresponds to the radius of spherical nucleus with equal volume. Considering axial symmetry and the reflection one with respect to the $z=0$ plane, $R(\vartheta,\varphi)$ can be further reduced as

$$R(\vartheta;\beta) = R_0\Big[1+\sqrt{\frac{5}{16\pi}}\beta\big(3\cos^2\vartheta-1\big)\Big], \tag{74}$$

where β describes the deformation of a nucleus deviated from the spherical shape, and the positive and negative values of β correspond to the prolate and oblate shapes, respectively. In the DWS potentials (71), the empirical radii $R^{\tau_3}_{\pm}$ shall be replaced by $R^{\tau_3}_{\pm}(\vartheta,\beta)$, leading to $\Sigma^{\tau_3}_{\pm} = \Sigma^{\tau_3}_{\pm}(r,\vartheta;\beta)$,

$$R^{\tau_3}_{\pm}(\vartheta;\beta) = R^{\tau_3}_{0,\pm}\Big[1+\sqrt{\frac{5}{16\pi}}\beta\big(3\cos^2\vartheta-1\big)\Big], \tag{75}$$

$$R^{\tau_3}_{0,\pm} = r^{\tau_3}_{0,\pm}A^{1/3}\Big(1-\frac{1}{3}\delta\Big)^{-2/3}\Big(1+\frac{2}{3}\delta\Big)^{-1/3}, \tag{76}$$

where $\delta = 3\sqrt{5/16\pi}\beta$, and the values of $r^{\tau_3}_{0,\pm}$ are given in Table I.

For the initial DWS potentials $\Sigma^{\tau_3}_{\pm}(r,\vartheta;\beta)$, similar expansion terms as the local self-energies in the Hartree energy functional (40) can be determined by

$$\Sigma^{\tau_3,\lambda_d}_{\pm}(r) = \int_0^{\pi}\Sigma^{\tau_3}_{\pm}(r,\vartheta)P_\lambda(\cos\vartheta)\sin\vartheta d\vartheta, \tag{77}$$

where the integration can be evaluated with the Gauss-Legendre algorithm. The initial matrix in the eigenvalue equation (52) is then obtained by replacing the expansion terms $\Sigma^{\lambda_d}_0 \pm \Sigma^{\lambda_d}_S$ in $H^D_{aa'}$ Eq. (55) with $\Sigma^{\tau_3,\lambda_d}_{\pm}$, since the kinetic part $H^{\rm kin}_{aa'}$ only depends on the DWS base and the nonlocal part $H^E_{aa'}$ is set as zero.

With the expansion of densities (38), it is rather straightforward to deduce the intrinsic multiple moment Q_{λ_d} for a deformed nucleus as

$$Q_{\lambda_d} = \sqrt{\frac{8}{2\lambda_d+1}}2\pi\int dr r^4\rho^{\lambda_d}_b(r), \tag{78}$$

and with obtained quadruple moment Q_2, the quadruple deformation β can be evaluated approximately by

$$\beta = \frac{\sqrt{5\pi}Q_2}{3R_0^2A}, \tag{79}$$

where $R_0 = 1.2A^{1/3}$.

III. RESULTS AND DISCUSSIONS

As the first attempt of the RHF calculations with the DWS base for an axially deformed nucleus, we first introduced the space truncation in this section. As the convergence check of the space truncations, we show the test calculations for the light ^{20}Ne, midheavy ^{56}Fe, and heavy Pb isotopes. Further we concentrate on the structure properties of ^{20}Ne described by the RHF Lagrangians PKOi, as compared to the calculations with the RMF Lagrangian DD-ME2 [114] and available experimental data.

A. Space truncations

Within the DDRHF theory, the calculations for axially deformed nuclei in this work are performed by applying the expansion of Dirac spinor on a spherical DWS base [66], i.e., Eq. (34). Related with that, two additional expansions shall be considered carefully, namely the decompositions of the propagators (30) in spherical coordinate (r,ϑ,φ) and the expansions of the coupling strengths in terms of Legendre functions (47). Thus, one needs to handle the truncations related to $(n\kappa)$ in Eq. (34), λ_y in Eq. (30), and λ_p in Eq. (47). In fact, these three truncations are not independent from each other. For a given λ_p in Eq. (47), the propagator's expansion λ_y is automatically truncated by the cutoff on $(n\kappa)$ in the spherical DWS base. Eventually, two independent truncations remain, namely the cutoffs on $(n\kappa)$ in expanding the Dirac spinors (34) and λ_p in expanding the density-dependent coupling strengths (47).

For the Dirac spinor $\psi_{\nu\pi m}$ with axial symmetry, in which the parity π and angular momentum projection m are good quantum numbers, the expansions (34) are carried with respect to the principle quantum number n and κ quantity on the spherical DWS base $\{\psi_{n\kappa m}\}$. For completeness, both positive and negative energy states of the spherical DWS base have to be taken into account. One should not mix this with the no-sea approximation adopted in the mean field approach, which corresponds to neglecting the Dirac sea in calculating the densities or currents. Notice that in expanding the Dirac spinors (34)-(35) the sum over the principle quantum number n is carried beforehand. Thus, for all the included κ blocks, the numbers of positive and negative energy states can be simply fixed as the same N_F and N_D values, respectively. One just needs to consider enough large N_F and N_D values, and such choice does not bring additional costs in the calculations, since the complicated nonlocal self-energies are independent on the principle quantum numbers ν or n (see the Appendix for details).

In general, the Dirac equation with the spherical DWS potentials are solved in a spherical box with the size R_m. To keep the numerical accuracy, the N_F value shall be modified with respect to R_m. In most of the cases, it is accurate enough to set R_m as 20 fm, and N_F and N_D are chosen as 28 and 10, respectively, and the accuracy has been verified in the RHFB calculations [67]. For the κ cutoff, we use K_m to denote the number of κ blocks

included in the expansion (34) of the Dirac spinor $\psi_{\nu\pi m}$ (28). In total, the number of the expansion terms in Eq. (34) is then $K_m \times (N_F + N_D)$.

For the open-shell nuclei, one needs to truncate the configuration space in evaluating the pairing effects. Practically, such truncation corresponds to the maximum values of m and ν of each m orbit. In this work, the finite-range Gogny force D1S is introduced as the pairing force such that the calculations can be smoothly converged with respect to the truncation. Thus, one can consider ν and m values as large as possible. For the former, it does not increase the numerical burden in calculating the Fock terms which are the dominant costs paid in the calculations. However, for the maximum m value $m_{\max}$, the computation costs can be enlarged by times when increasing $m_{\max}$.

In order to unify the cutoffs and reduce the numerical complexity, we set the maximum m value as $m_{\max}$ and the number of κ blocks considered in expanding the Dirac spinor $\psi_{\nu\pi m_{\max}}$ is set as $K_{m_{\max}}$, which gives the maximum absolute κ value as $k_{\max} = m_{\max} + K_{m_{\max}} - 1/2$. Hence, for an arbitrary Dirac spinor $\psi_{\nu\pi m}$, the κ quantities in the expansion (34) include $|\kappa| = m + 1/2$, $m + 3/2$, $\cdots$, $k_{\max}$ and $\mathrm{sign}(\kappa) = \pi * (-1)^{|\kappa|}$, $\pi = \pm 1$ being positive and negative parities, respectively.

For a given nucleus, the $m_{\max}$ value is usually determined by the convergence requirement of the BCS pairing. Practically, both the $m_{\max}$ and $k_{\max}$ (or $K_{m_{\max}}$) values are decided by a careful convergence check. For instance, in the case of large deformation, some orbits containing the components with large κ values may intrude even across the well-known major shells. Thus, one needs to enlarge $m_{\max}$ and $K_{m_{\max}}$ values, which can remarkably increase the computational cost.

For the density-dependent coupling strengths (47), the λ_p value shall be an even integer starting from 0 because of the axial symmetry and parity conservation. In general, it is accurate enough to have four terms $\lambda_p = 0, 2, 4, 6$ for most of the nuclei. Thus, with fixed truncation in expanding the Dirac spinor, the cutoff on the λ_y value in decomposing the propagators (30) is automatically determined as $\lambda_y^{\max} = 2k_{\max} + \lambda_p^{\max}$.

B. Convergence check

At first, we take the light nucleus ^{20}Ne as an example of the convergence check. Figure 2 shows the binding energy [plot (a)] and the quadruple deformation β [plot (b)] as referred to the m-cutoff $m_{\max}$, in which $K_{m_{\max}}$ is fixed as 3. In Fig. 2(a), it is seen that the binding energies converge when $m_{\max} \geq 9/2$, as well as the deformation parameter β shown in Fig. 2(b). On the other hand, it is also shown that with different initial deformation β_0, the calculations converge to the local minimum nearby. One may notice that with $m_{\max} = 3/2$, the calculations with $\beta_0 = 0$ and 0.5 give the same binding energies. For ^{20}Ne with spherical symmetry, the last occupied orbits are $d_{5/2}$ which exceed $m_{\max} = 3/2$. Thus, the calculations with $\beta_0 = 0$ can not converge to spherical shape. Considering the convergence of the binding energy and deformation, it is precise enough to choose $m_{\max} = 11/2$ and $K_{m_{\max}} = 3$ for ^{20}Ne.

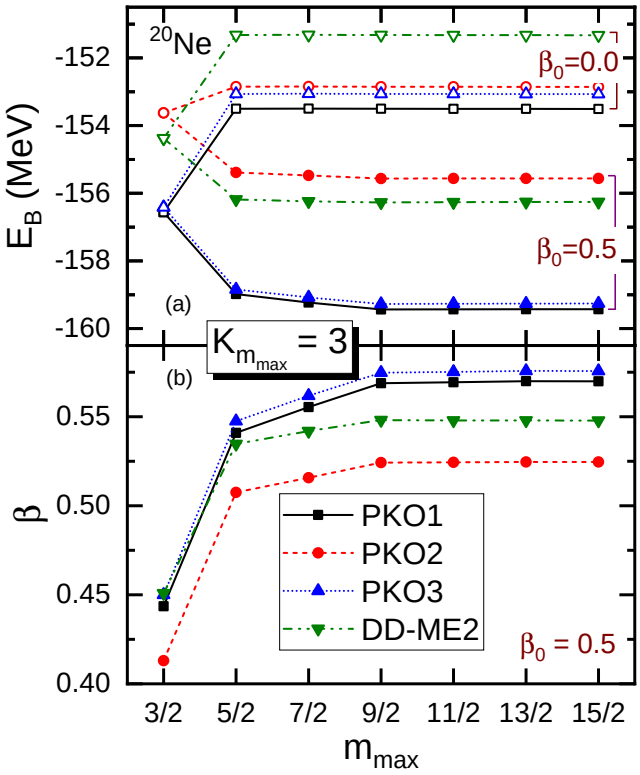

FIG. 1. (Color online) Binding energy E_B (MeV) (a) and quadruple deformation β (b) of ^{20}Ne calculated by PKOi and DD-ME2 with respect to $m_{\max}$, in which $K_{m_{\max}}$ is fixed as 3. The open symbols denote the calculations with the initial deformation $\beta_0 = 0$ and the filled ones for $\beta_0 = 0.5$.

Here, we only show the convergence check with respect to $m_{\max}$. For the expansion of the density-dependent coupling strength, $\lambda_p^{\max}$ has been checked for the nuclei with a wide range of mass numbers, and it is enough to choose $\lambda_p^{\max} = 6$ for most of nuclei. For the $K_{m_{\max}}$ value, it is accurate enough to fix $K_{m_{\max}} = 3$ with appropriate $m_{\max}$ value that is in general decided by the configuration space of the pairing correlations. For economical reasons, one can carefully choose an appropriate combination of the $m_{\max}$ and $K_{m_{\max}}$ values.

We further check the convergence for the medium-heavy nuclei, here, taking ^{56}Fe as an example. In Table II is shown the binding energy E_B (MeV), the total, neutron, and proton quadruple deformations β, β_n, and β_p with respect to the m-cutoff $m_{\max}$, in which $K_{m_{\max}}$ is set as 3 and $\beta_0 = 0.3$. It is seen that for both PKO1 and PKO2, the calculations are converged after $m_{\max} \geq 11/2$. Even in the cases with $m_{\max} < 11/2$, the results are rather close to the converged ones. It is similar to the calculations of ^{20}Ne with $\beta_0 = 0.0$,

which converge quickly when $m_{\max} \geq 5/2$. This is due to the reason that with small deformation or spherical shape, the contributions from high κ blocks contribute little to the expansion of the Dirac spinor $\psi_{\nu\pi m}$ whereas with large deformation, e.g., the calculations of ^{20}Ne with $\beta_0 = 0.5$ in Fig. 1, the components with large κ values may have substantial contributions.

TABLE II. Binding energy E_B (MeV), quadruple deformation β (the total), β_n (neutron), β_p (proton) of ^{56}Fe calculated by PKO1 and PKO2 with respect to $m_{\max}$, in which $K_{m_{\max}}$ is fixed as 3 and the initial deformation $\beta_0 = 0.3$. Notice that $E_B^{\exp} = -492.26$ MeV [115] and $\beta^{\exp} = 0.25$ [116].

	PKO1				PKO2			
$m_{\max}$	E_B	β	β_n	β_p	E_B	β	β_n	β_p
7/2	−489.9	0.24	0.24	0.24	−489.3	0.22	0.22	0.22
9/2	−489.9	0.24	0.24	0.24	−489.4	0.22	0.23	0.22
11/2	−490.0	0.24	0.24	0.24	−489.4	0.23	0.23	0.22
13/2	−490.0	0.24	0.24	0.24	−489.4	0.23	0.23	0.22
15/2	−490.0	0.24	0.24	0.24	−489.4	0.23	0.23	0.22

For the heavy nuclei, we take the even Pb isotopes from ^{182}Pb to ^{214}Pb as examples for the convergence check. Table III shows the binding energies calculated by PKOi and DD-ME2, and the experimental (exp) values [115] and the results calculated with the spherical code (Sph.) are also given as the references. For the calculations with deformed (Def.) code, $m_{\max}$ is set as 15/2 and $K_{m_{\max}} = 3$. Notice that in both Sph. and Def. calculations the pairing correlations are treated with the BCS method by taking the Gogny force D1S as the pairing force. For all the selected isotopes, the Def. calculations with $\beta_0 = 0$ give the spherical shape. It can be seen that the deviations between the Def. and Sph. calculations are rather tiny (dozens of keV), particularly for the doubly magic ^{208}Pb, which in fact illustrates the accuracy of the Def. code in calculating the heavy nuclei. For the open-shell Pb isotopes, the accuracies are as perfect as the doubly magic ^{208}Pb, and the relative deviations are usually less than 0.01%. For the matter radii, a similar accuracy can be also obtained by the Def. code, which is not shown for simplicity.

As a further example of the convergence check, we choose the heavier nucleus ^{220}Rn that has the reported experimental quadruple deformation as $\beta = 0.1269$ [117]. It is worthwhile to notice that for the heavy nuclei the truncations of the expansions (34) and (47) shall be tested carefully. Here, we take five terms $\lambda_p = 0, 2, 4, 6, 8$ in expanding the density-dependent coupling strengths (47) for ^{220}Rn. Using PKO1 and DD-ME2, the convergence tests with respect to $m_{\max}$ are shown in Table IV, including the binding energy E_B, matter and charge radii r and r_{ch}, and quadruple deformations (β, β_n, β_p). As shown in Table IV, both RHF (PKO1) and RMF (DD-ME2) calculations show appropriate convergence with respect to $m_{\max}$, which has illustrated the reliability of the expansion on the DWS base. Moreover, both RHF and RMF Lagrangians provide a reasonable description on the bulk properties of ^{220}Rn, referring the available data.

C. Description of ^{20}Ne

After a careful convergence check, we performed systematical calculations for ^{20}Ne, a typically deformed nucleus. First, we show the constraint calculation with respect to the quadruple deformation β for ^{20}Ne in Fig. 2, where the space truncations are set as $m_{\max} = 11/2$ and $K_{m_{\max}} = 3$ and the filled cycles denote the local minima. For comparison, we employed the RHF Lagrangians PKOi and the RMF one DD-ME2 [114].

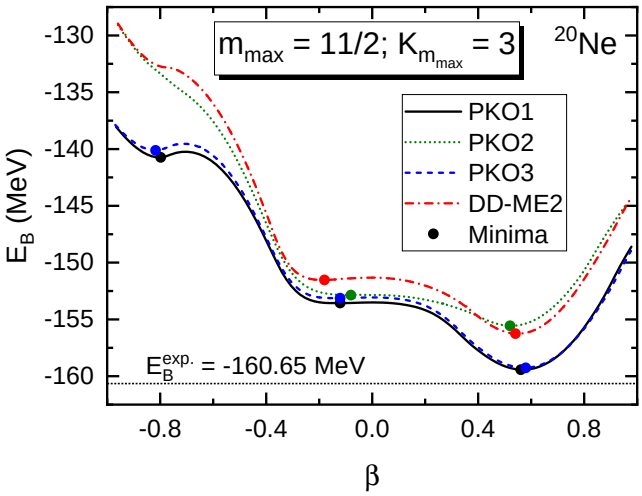

FIG. 2. (Color online) Binding energy E_B (MeV) as a function of deformation β for ^{20}Ne. The results are calculated by PKOi and DD-ME2 with $m_{\max} = 11/2$ and $K_{m_{\max}} = 3$. The filled circles denote the local minima.

For ^{20}Ne as shown in Fig. 2, the RHF Lagrangians PKO1 and PKO3, which contain the π-PV coupling, present rather similar results. In contrast, the RHF Lagrangian PKO2 and RMF one DD-ME2 give systematically less bound results. Referring to the experimental value of the binding energy of ^{20}Ne, it can be seen that PKO1 and PKO3 show nice agreement, and the results given by PKO2 and DD-ME2 are less bound and the deviations are $\approx$ 5 MeV. It shall be mentioned that there exists some discrepancy on the binding energies between our results and the ones in Ref. [104] (Figs. 1 and 9 therein). For the RMF Lagrangian DD-ME2, our results are coincident with the calculations using the code developed from Ref. [65], while showing about 1.5 MeV less than the one in Ref. [104]. Moreover, for the RHF Lagrangian PKO2, the calculations in Ref. [104] (Fig. 1 therein) only present nearly converged results for ^{20}Ne, showing similar deviation from our calculations as DD-ME2. The possible reason might be due to the fact that stronger pairing effects are obtained by the general Bogoliubov

TABLE III. Binding energies of Pb isotopes with even neutron numbers form $N = 100$ to 132, calculated with spherical (Sph.) and axially deformed (Def.) RHF codes. The results are calculated with the RHF Lagrangians PKOi and the RMF one DD-ME2, in comparison to the experimental data [115].

A	Exp.	PKO1		PKO2		PKO3		DD-ME2	
		Sph.	Def.	Sph.	Def.	Sph.	Def.	Sph.	Def.
182	−1411.65	−1411.76	−1411.80	−1411.94	−1412.13	−1412.61	−1412.64	−1409.81	−1409.88
184	−1432.02	−1431.28	−1431.31	−1431.78	−1431.98	−1432.09	−1432.11	−1429.22	−1429.31
186	−1451.80	−1450.32	−1450.34	−1451.18	−1451.38	−1451.07	−1451.08	−1448.12	−1448.21
188	−1471.07	−1468.94	−1468.97	−1470.16	−1470.35	−1469.63	−1469.64	−1466.66	−1466.77
190	−1489.81	−1487.19	−1487.22	−1488.73	−1488.92	−1487.82	−1487.83	−1484.91	−1485.01
192	−1508.10	−1505.09	−1505.15	−1506.91	−1507.08	−1505.68	−1505.70	−1502.90	−1503.01
194	−1525.89	−1522.68	−1522.75	−1524.69	−1524.84	−1523.23	−1523.26	−1520.65	−1520.75
196	−1543.17	−1539.97	−1540.05	−1542.06	−1542.19	−1540.48	−1540.52	−1538.18	−1538.27
198	−1560.04	−1556.97	−1557.04	−1559.01	−1559.11	−1557.44	−1557.49	−1555.48	−1555.55
200	−1576.36	−1573.67	−1573.71	−1575.52	−1575.61	−1574.12	−1574.17	−1572.54	−1572.61
202	−1592.19	−1590.04	−1590.06	−1591.58	−1591.65	−1590.48	−1590.53	−1589.35	−1589.40
204	−1607.51	−1606.03	−1606.05	−1607.15	−1607.20	−1606.50	−1606.53	−1605.87	−1605.91
206	−1622.32	−1621.54	−1621.55	−1622.11	−1622.13	−1622.04	−1622.06	−1622.00	−1622.02
208	−1636.43	−1636.29	−1636.29	−1636.00	−1636.01	−1636.80	−1636.81	−1637.39	−1637.40
210	−1645.55	−1644.26	−1644.23	−1643.54	−1643.55	−1644.79	−1644.77	−1644.19	−1644.20
212	−1654.52	−1652.13	−1652.04	−1650.98	−1650.99	−1652.65	−1652.59	−1651.00	−1651.01
214	−1663.29	−1659.88	−1659.74	−1658.31	−1658.30	−1660.35	−1660.26	−1657.82	−1657.83

TABLE IV. Binding energy E_B (MeV), quadruple deformations (β, β_n, β_p), matter and charge radii r and r_{ch} (fm) of ^{220}Rn calculated by PKO1 (upper panel) and DD-ME2 (lower panel) with respect to $m_{\max}$, in which $K_{m_{max}} = 3$, $\lambda_p = 0, 2, 4, 6, 8$, and the initial deformation $\beta_0 = 0.2$. Notice that $E_B^{\exp} = -1697.796$ MeV [115] and $\beta^{\exp} = 0.1269$ [117].

$m_{\max}$	E_B	r	r_{ch}	β	β_n	β_p
13/2	−1696.27	5.753	5.659	0.1241	0.1275	0.1189
15/2	−1696.89	5.755	5.661	0.1297	0.1330	0.1246
17/2	−1697.20	5.757	5.663	0.1334	0.1369	0.1280
19/2	−1697.28	5.758	5.663	0.1345	0.1381	0.1290
13/2	−1694.75	5.726	5.656	0.1237	0.1273	0.1182
15/2	−1695.17	5.728	5.658	0.1271	0.1305	0.1217
17/2	−1695.34	5.729	5.659	0.1287	0.1322	0.1232
19/2	−1695.36	5.729	5.659	0.1288	0.1323	0.1233

TABLE V. Deformations (β, β_n, β_p), binding energies E_B (MeV), and matter radii r (fm) and charge radii r_{ch} (fm) of ^{20}Ne at local minima given by PKOi ($i = 1, 2, 3$) and DD-ME2. Notice that $E_B^{\exp} = -160.65$ MeV [115].

	E_B	β	β_n	β_p	r	r_{ch}
PKO1	−140.74	−0.798	−0.791	−0.805	3.054	3.168
	−153.56	−0.121	−0.117	−0.124	2.745	2.873
	−159.43	0.561	0.554	0.567	2.820	2.943
PKO3	−140.12	−0.817	−0.810	−0.824	3.081	3.194
	−153.13	−0.121	−0.118	−0.124	2.755	2.883
	−159.26	0.580	0.573	0.586	2.835	2.958
PKO2	−152.86	−0.080	−0.077	−0.084	2.726	2.855
	−155.56	0.520	0.514	0.527	2.791	2.915
DD-ME2	−151.53	−0.180	−0.176	−0.184	2.764	2.895
	−156.26	0.541	0.533	0.548	2.813	2.940

method [104] than the BCS method [118]. The local minima extracted from Fig. 2 are summarized in Table V. Within the range $\beta \in (-1.0, 1.0)$, there exist three local minima in the PKO1 and PKO3 results: a stable and strongly deformed prolate, a soft oblate, and a high-lying and largely deformed oblate. For the formal two prolate and oblate shapes, PKO2 and DD-ME2 present rather similar deformations, while the largely deformed oblate is not supported.

From Table V and Fig. 2, one can see that the selected effective Lagrangians give similar binding energies on the oblate minima [$\beta \sim (-0.1, -0.2)$] of ^{20}Ne, particularly for the RHF ones PKOi. When approaching the prolate minima, the ground state of ^{20}Ne, the deviations between PKO2 and PKO1 (PKO3) become more and more notable. Eventually, PKO1 and PKO3, which contain the π-PV coupling, show much better agreement with the experimental data of the binding energy of ^{20}Ne [115].

In order to understand the deviations between PKO2 and PKO1 (PKO3), we show the evolution of neutron (left panel) and proton (right panel) single particle energies with respect to the quadruple deformation $\beta \in [0, 0.6)$ in Fig. 3, where the notation $\nu[m]\pi$ is introduced to denote the orbits. It can be seen that both

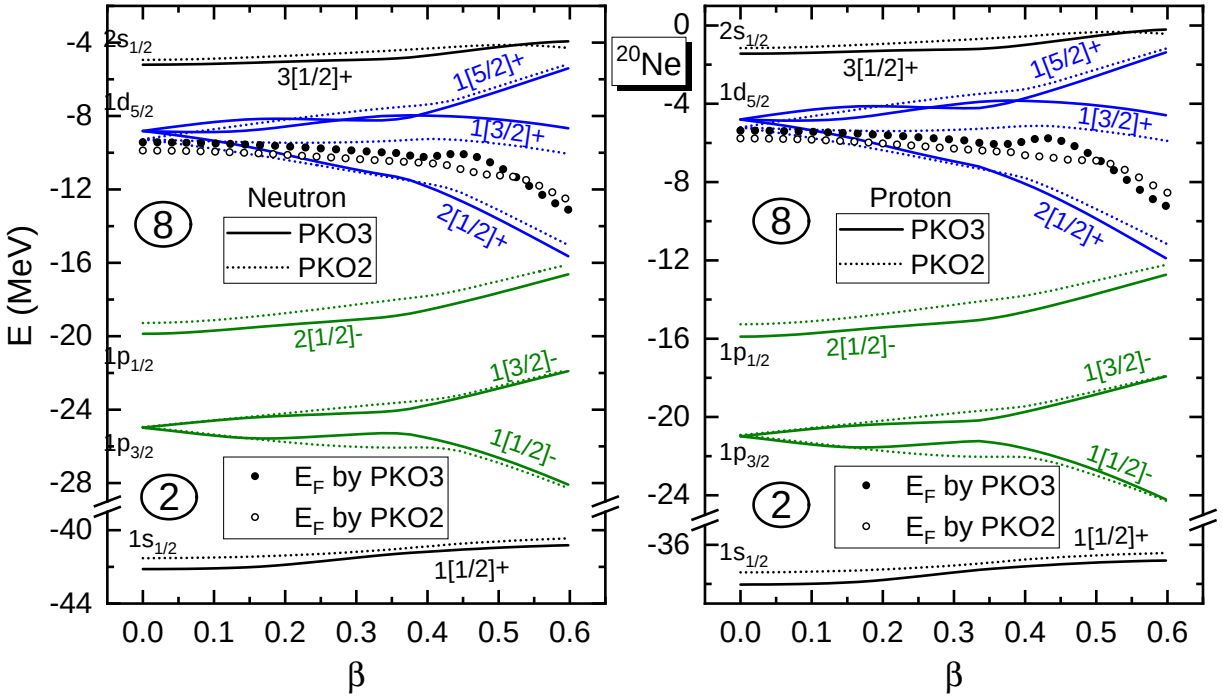

FIG. 3. (Color online) Evolution of neutron (left panel) and proton (right panel) single particle energies given by PKO2 (dotted lines) and PKO3 (solid lines) for ^{20}Ne with respect to the deformation $\beta \in [0, 0.6)$, in which the filled and open circles denote the Fermi energies E_F given by PKO3 and PKO2, respectively.

neutron and proton single-particle energies show similar systematical evolutions with respect to β. Following the shape evolution, both neutron and proton spherical shells $N/Z = 8$ are continuously reduced and eventually the deformed ones $N/Z = 10$ emerge at rather large β values. In general, the orbits, which are branched from the same degenerated spherical orbits nlj ($j \geqslant 3/2$), will deviate from each other with respect to the deformation β. As seen from the PKO2 results (dotted lines), the orbits $2[1/2]+$ and $1[1/2]-$ with the smallest m values, respectively branched from the spherical $1d_{5/2}$ and $1p_{3/2}$ states, tend to be more and more bound, whereas the ones $1[5/2]+$ and $1[3/2]-$ with the largest m values become less and less bound, along the shape evolution from the spherical to prolate. This in fact reflects the typical deformation effects.

However, comparing to the results given by PKO3 which contains the π-PV coupling [78], the situation can be notably different. As shown in Fig. 3, PKO3 (solid lines) and PKO2 (dotted lines) present different systematics on the shape evolution of the valence orbits branched from the degenerated spherical one $1d_{5/2}$. In order to understand the effects of the π-PV coupling, Fig. 4 shows the splittings between valence neutron orbits $2[1/2]+$ and $1[3/2]+$, namely $\Delta E = E_{1[3/2]+} - E_{2[1/2]+}$ (MeV), with respect to the quadruple deformation β, and the inset shows the effective neutron pairing gap Δ_n (MeV) as functions of β. It can be seen that following the shape evolution from the spherical to the prolate, PKO3 (solid line) presents notably larger splittings ΔE than PKO2 (dotted line), and the enhancements from PKO2 to PKO3 are almost fully due to the contributions from the π-PV coupling (in grid pattern).

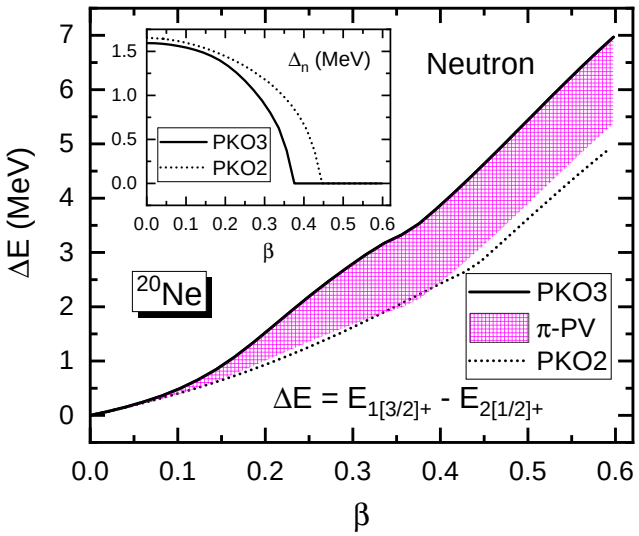

FIG. 4. (Color online) Splittings (MeV) between neutron valence orbits $2[1/2]+$ and $1[3/2]+$ given by PKO3 (solid line) and PKO2 (dotted line), namely $\Delta E = E_{1[3/2]+} - E_{2[1/2]+}$, with respect to the deformation $\beta \in [0, 0.6)$ for ^{20}Ne, where the grid pattern denotes the contributions from the π-PV coupling in PKO3. The inset shows the neutron pairing gaps Δ_n (MeV) as functions of β given by PKO3 and PKO2.

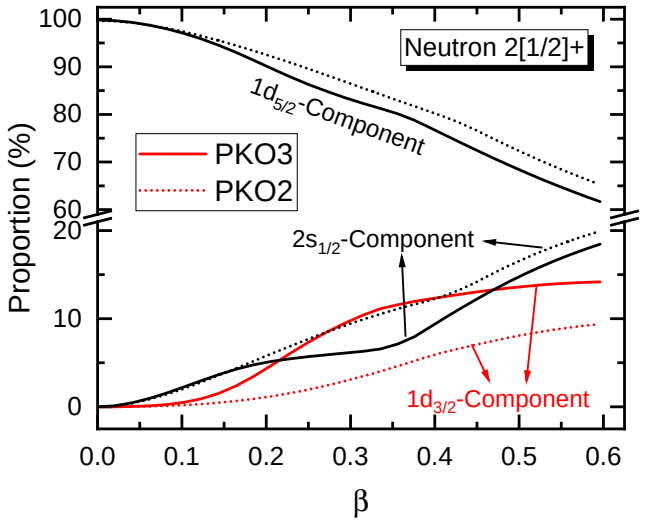

FIG. 5. (Color online) Proportions (in percentage) of the main components in expanding the neutron $2[1/2]+$ orbit for ^{20}Ne with respect to the deformation $\beta \in [0, 0.6]$, namely the $1d_{5/2}$, $2s_{1/2}$, and $1d_{3/2}$ components. The results are given by PKO3 (solid lines) and PKO2 (dotted lines).

Qualitatively, one can understand such enhancement from the nature of the tensor force carried by the π-PV coupling in PKO3 [78, 90], which leads to repulsive/attractive couplings between the κ components with the same/opposite signs [119]. As a supplement, we show in Fig. 5 the proportions (in percentage) of the main expansion components [see Eq. (29)] as functions of the deformation β for the neutron orbit $2[1/2]+$, namely the κ components $1d_{5/2}$ ($\kappa = -3$), $1d_{3/2}$ ($\kappa = 2$), and $2s_{1/2}$ ($\kappa = -1$). For both PKO2 (dotted lines) and PKO3 (solid lines), the negative κ component $1d_{5/2}$ dominates the expansion of the Dirac spinor (more than 60%). In fact, for another two neutron orbits $1[3/2]+$ and $1[5/2]+$, which are not shown for simplicity, the negative κ component $1d_{5/2}$ plays a compressively dominant role (more than 90%). Similar situation can be also found in expanding the proton orbits. If looking at the core configurations of both neutron and proton ($N, Z = 8$), only one orbit $2[1/2]-$ can be dominated by the positive κ components $1p_{1/2}$ ($\kappa = 1$), and the other three ($1[1/2]+$, $1[1/2]-$, and $1[3/2]-$) contain mainly the negative κ components, which indicates the core exhibiting as the negative κ components in total. Thus, the tensor force components carried by the π-PV coupling in PKO3 presents additional repulsive interactions between the core and valance orbits $2[1/2]+$, $1[3/2]+$, and $1[5/2]+$.

However, for the orbit $2[1/2]+$, the proportions of the positive κ component $1d_{3/2}$ ($\kappa = 2$) are notable, which are largely enhanced from PKO2 to PKO3 following the shape evolution. In contrast to the negative κ component $1d_{5/2}$, the tensor couplings between the positive κ component $1d_{3/2}$ and the core, that behaves like negative κ components, are attractive, which tends to make ^{20}Ne more bound. Comparing to the orbits $1[3/2]+$ and $1[5/2]+$, the repulsive tensor couplings between the orbit $2[1/2]+$ and the core are then notably reduced by enhanced proportions of the positive κ component $1d_{3/2}$, from which one can understand well the enhanced splittings ΔE from PKO2 to PKO3 in Fig. 4, as well as more bound ground state given by PKO3 than PKO2 in Fig. 2.

On the other hand, via the π-PV coupling, the core of ^{20}Ne can be also polarized differently by the valence nucleons in the PKO2 and PKO3 calculations, manifested as notably different compositions of the valence orbit $2[1/2]+$ in Fig. 5. It is thus expected that the mean field described by PKO2 and PKO3 can be notably different. As the direct evidences, not only presenting different compositions of the valence orbit $2[1/2]+$, PKO2 and PKO3 also give distinctively different systematics on the shape evolutions of the orbits $1[3/2]+$ and $1[5/2]+$, see Fig. 3. Coincidentally, one may also find some similarity on the shape evolutions of the orbits $1[3/2]+$ and $1[5/2]+$, and those of the $2s_{1/2}$ and $1d_{3/2}$ proportions for the orbit $2[1/2]+$, see Figs. 3 and 5. To some extent, such similarity might illustrate the consistent relation between the systematics of the orbits $1[3/2]+$ and $1[5/2]+$ and the core polarization by the valence nucleons occupying the orbit $2[1/2]+$. It shall be noticed that the shape evolution of the orbits $1[3/2]+$ and $1[5/2]+$ cannot be attributed directly to the role of the tensor force, because both orbits are similarly dominated by the negative κ component $1d_{5/2}$. Moreover, the pairing correlations may not play a substantial role in interpreting the systematic difference between PKO2 and PKO3, since both show similar pairing effects, as seen from the inset of Fig. 4.

IV. SUMMARY

In this paper, the axially deformed relativistic Hartree-Fock (RHF) model is established by utilizing the spherical Dirac Woods-Saxon (DWS) base that can probably describe the asymptotic behavior of wave functions. The formalism of the axially deformed RHF model based on spherical DWS base is presented in details, as well as the relevant space truncations. Taking the light ^{20}Ne, midheavy ^{56}Fe, and heavy Pb isotopes as the candidates, the reliability of the expansions are illustrated, as well as the verification of the accuracy of the deformed RHF codes.

The axially deformed RHF model based on the spherical DWS base is applied preliminarily to study the structure properties of ^{20}Ne, a typically deformed nucleus, with the RHF effective Lagrangian PKOi and RMF ones DD-ME2. It is found that the RHF Lagrangians PKO1 and PKO3, which contain the π-pseudovector coupling, improve the description of the binding energy of ^{20}Ne. Furthermore, the discussions on the systematics of the shape evolution of single-particle energies indicate that the π-PV coupling, mainly

the tensor force component, may present notable effects in determining the shape evolution of nucleus, as well as the polarization of the core of nucleus. Thus, as perspectives, it is valuable for investigating the effects of the Fock terms, especially the π-PV and ρ-T couplings, in determining the structure properties of the deformed nuclei, which deserves further systematical investigations with the existing RHF Lagrangians PKOi and PKA1.

ACKNOWLEDGMENTS

This work was partly supported by the Strategic Priority Research Program of Chinese Academy of Sciences, Grant No. XDB34000000, and by the Natural Science Foundation of China under Grant Nos. 11675065, 11875152, and 11905088, and by the Supercomputer Center of HIRFL, Lanzhou. The authors acknowledge fruitful discussions with the colleagues in Institute of Modern Physics.

[1] C. Sturm, B. Sharkov, and H. Stöker, Nucl. Phys. A **834**, 682c (2010).
[2] M. Thoennessen, Nucl. Phys. A **834**, 688c (2010).
[3] W. L. Zhan, H. S. Xu, G. Q. Xiao, J. W. Xia, H. W. Zhao, Y. J. Yuan, and H.-C. Groupa, Nucl. Phys. A **834**, 694c (2010).
[4] T. Motobayashi, Nucl. Phys. A **834**, 707c (2010).
[5] S. Gales, Nucl. Phys. A **834**, 717c (2010).
[6] B. Jonson, Phys. Rep. **389**, 1 (2004).
[7] I. Tanihata, Prog. Part. Nucl. Phys. **35**, 505 (1995).
[8] A. S. Jensen, K. Riisager, D. V. Fedorov, and E. Garrido, Rev. Mod. Phys **76**, 215 (2004).
[9] R. F. Casten and B. M. Sherrill, Prog. Part. Nucl. Phys. **45**, S171 (2000).
[10] S. N. Ershov, L. V. Grigorenko, J. S. Vaagen, and M. V. Zhukov, J. Phys. G: Nucl. Phys. **37**, 064026 (2010).
[11] C. R. Hoffman, T. Baumann, D. Bazin, J. Brown, G. Christian, P. A. DeYoung, J. E. Finck, N. Frank, J. Hinnefeld, R. Howes, et al., Phys. Rev. Lett. **100**, 152502 (2008).
[12] H. Simon, D. Aleksandrov, T. Aumann, L. Axelsson, T. Baumann, M. J. G. Borge, L. V. Chulkov, R. Collatz, J. Cub, W. Dostal, et al., Phys. Rev. Lett. **83**, 496 (1999).
[13] T. Motobayashi, Y. Ikeda, Y. Ando, K. Ieki, M. Inoue, N. Iwasa, T. Kikuchi, M. Kurokawa, S. Moriya, S. Ogawa, et al., Phys. Lett. B. **346**, 9 (1995).
[14] K. Tshoo, Y. Satou, H. Bhang, S. Choi, T. Nakamura, Y. Kondo, S. Deguchi, Y. Kawada, N. Kobayashi, Y. Nakayama, et al., Phys. Rev. Lett. **109**, 022501 (2012).
[15] A. Ozawa, T. Kobayashi, T. Suzuki, K. Yoshida, and K. Y. I. Tanihata, Phys. Rev. Lett. **84**, 5493 (2000).
[16] R. Kanungo, C. Nociforo, A. Prochazka, T. Aumann, D. Boutin, D. Cortina-Gil, B. Davids, M. Diakaki, F. Farinon, H. Geissel, et al., Phys. Rev. Lett. **102**, 152501 (2009).
[17] A. Gade, R. V. F. Janssens, D. Bazin, R. Broda, B. A. Brown, C. M. Campbell, M. P. Carpenter, J. M. Cook, A. N. Deacon, D.-C. Dinca, et al., Phys. Rev. C **74**, 021302(R) (2006).
[18] D. Steppenbeck, S. Takeuchi, N. Aoi, P. Doornenbal, M. Matsushita, H. Wang, Y. Utsuno, H. Baba, S. Go, J. Lee, et al., Phys. Rev. Lett. **114**, 252501 (2015).
[19] D. Steppenbeck, S. Takeuchi, N. Aoi, P. Doornenbal, M. Matsushita, H. Wang, H. Baba, N. Fukuda, S. Go, M. Honma, et al., Nature **502**, 207 (2013).
[20] T. Minamisono, T. Ohtsubo, I. Minami, S. Fukuda, A. Kitagawa, M. Fukuda, K. Matsuta, Y. Nojiri, S. Takeda, H. Sagawa, et al., Phys. Rev. Lett. **69**, 2058 (1992).
[21] I. Tanihata, H. Hamagaki, O. Hashimoto, Y. Shida, N. Yoshikawa, K. Sugimoto, O. Yamakawa, T. Kobayashi, and N. Takahashi, Phys. Rev. Lett. **55**, 2676 (1985).
[22] W. Schwab, H. Geissel, H. Lenske, K.-H. Behr, A. Brünle, K. Burkard, H. Irnich, T. Kobayashi, G. Kraus, A. Magel, et al., Z. Phys. A **350**, 283 (1995).
[23] W. Gordy, Phys. Rev. **76**, 139 (1949).
[24] C. H. Townes, H. M. Foley, and W. Low, Phys. Rev. **76**, 1415 (1949).
[25] R. D. Hill, Phys. Rev. **76**, 998 (1949).
[26] J. Rainwater, Phys. Rev. **79**, 432 (1950).
[27] A. Bohr, Phys. Rev. **81**, 134 (1951).
[28] A. Bohr and B. R. Mottelson, Phys. Rev. **89**, 316 (1953).
[29] A. Bohr and B. R. Mottelson, Phys. Rev. **90**, 717 (1953).
[30] N. Bohr and F. Kalckar, K. Dan. Vidensk. Selsk. Mat. Fys. Medd. **14**, 10 (1937).
[31] P. Campbell, I. D. Moore, and M. R. Pearson, Prog. Part. Nucl. Phys. **86**, 127 (2016).
[32] B. Cheal and K. T. Flanagan, J. Phys. G: Nucl. Part. Phys. **37**, 113101 (2010).
[33] D. E. Alburger, C. Chasman, K. W. Jones, J. W. Olness, and R. A. Ristinen, Phys. Rev **136**, B916 (1964).
[34] H. L. Crawford, P. Fallon, A. O. Macchiavelli, P. Doornenbal, N. Aoi, F. Browne, C. M. Campbell, S. Chen, R. M. Clark, M. L. Cortés, et al., Phys. Rev. Lett. **122**, 052501 (2019).
[35] D. S. Ahn, N. Fukuda, H. Geissel, N. Inabe, N. Iwasa, T. Kubo, K. Kusaka, D. J. Morrissey, D. Murai, T. Nakamura, et al., Phys. Rev. Lett. **123**, 212501 (2019).
[36] S. M. Lenzi, F. Nowacki, A. Poves, and K. Sieja, Phys. Rev. C **82**, 054301 (2010).
[37] P. E. Garrett, T. R. Rodríguez, A. D. Varela, K. L. Green, J. Bangay, A. Finlay, R. A. E. Austin, G. C. Ball, D. S. Bandyopadhyay, V. Bildstein, et al., Phys. Rev. Lett. **123**, 142502 (2019).

[38] L. Gaudefroy, J. M. Daugas, M. Hass, S. Grévy, C. Stodel, J. C. Thomas, L. Perrot, M. Girod, B. Rossé, J. C. Angélique, et al., Phys. Rev. Lett. **102**, 092501 (2009).

[39] T. Togashi, Y. Tsunoda, T. Otsuka, and N. Shimizu, Phys. Rev. Lett. **117**, 172502 (2016).

[40] A. Oberstedt, S. Oberstedt, M. Gawrys, and N. Kornilov, Phys. Rev. Lett. **99**, 042502 (2007).

[41] T. Ichikawa, J. A. Maruhn, N. Itagaki, and S. Ohkubo, Phys. Rev. Lett. **107**, 112501 (2011).

[42] H. Yukawa, Proc. Phys. Math. Soc. Japan **17**, 48 (1935).

[43] P.-G. Reinhard, Reports on Progress in Physics **52**, 439 (1989).

[44] P. Ring, Prog. Part. Nucl. Phys. **37**, 193 (1996).

[45] M. Bender, P.-H. Heenen, and P.-G. Reinhard, Revs. Mod. Phys. **75**, 121 (2003).

[46] D. Vretenar, A. V. Afanasjev, G. A. Lalazissis, and P. Ring, Phys. Rep. **409**, 101 (2005).

[47] J. Meng, H. Toki, S. G. Zhou, S. Q. Zhang, W. H. Long, and L. S. Geng, Prog. Part. Nucl. Phys. **57**, 470 (2006).

[48] T. Nikšić, D. Vretenar, and P. Ring, Prog. Part. Nucl. Phys **66**, 519 (2011).

[49] H. Liang, J. Meng, and S.-G. Zhou, Phys. Rep. **570**, 1 (2015).

[50] J. D. Walecka, Ann. Phys. (NY) **83**, 491 (1974).

[51] J. Geng, J. J. Li, W. H. Long, Y. F. Niu, and S. Y. Chang, Phys. Rev. C **100**, 051301(R) (2019).

[52] J. Boguta and A. R. Bodmer, Nucl. Phys. **A 292**, 413 (1977).

[53] Y. Sugahara and H. Toki, Nucl. Phys. **A 579**, 557 (1994).

[54] W. H. Long, J. Meng, N. Van Giai, and S.-G. Zhou, Phys. Rev. **C 69**, 034319 (2004).

[55] R. Brockmann and H. Toki, Phys. Rev. Lett. **68**, 3408 (1992).

[56] H. Lenske and C. Fuchs, Phys. Lett. **B 345**, 355 (1995).

[57] C. Fuchs, H. Lenske, and H. H. Wolter, Phys. Rev. C **52**, 3043 (1995).

[58] S. Typel and H. H. Wolter, Nucl. Phys. **A 656**, 331 (1999).

[59] M. G. Mayer, Phys.Rev **75**, 1969 (1949).

[60] O. Haxel, J. H. D. Jensen, and H. E. Suess, Phys.Rev **75**, 1766 (1949).

[61] J. N. Ginocchio, Phys. Rev. Lett. **78**, 436 (1997).

[62] J. Meng, K. Sugawara-Tanabe, S. Yamaji, P. Ring, and A. Arima, Phys. Rev. C **58**, R628 (1998).

[63] W. Pannert, P. Ring, and J. Boguta, Phys. Rev. Lett. **59**, 2420 (1987).

[64] C. E. Price and G. E. Walker, Phys. Rev. **C.36**, 354 (1987).

[65] Y. K. Gambhir, P. Ring, and A. Thimet, Ann. Phys. (NY) **198**, 132 (1990).

[66] S.-G. Zhou, J. Meng, and P. Ring, Phys. Rev. C **68**, 034323 (2003).

[67] W. H. Long, P. Ring, N. Van Giai, and J. Meng, Phys. Rev. **C 81**, 024308 (2010).

[68] S. G. Zhou, J. Meng, S. Yamaji, and S. C. Yang, Chin Phys Lett. **17**, 717 (2000).

[69] M. Stoitsov, P. Ring, D. Vretenar, and G. A. Lalazissis, Phys. Rev. C **58**, 2086 (1998).

[70] M. V. Stoitsov, W. Nazarewicz, and S. Pittel, Phys. Rev. C **58**, 2092 (1998).

[71] M. V. Stoitsov, J. Dobaczewski, P. Ring, and S. Pittel, Phys. Rev. C **61**, 034311 (2000).

[72] W. Koepf and P. Ring, Z. Phys. A **339**, 81 (1991).

[73] R. D. Woods and D. S. Saxon, Phys. Rev. **95**, 577 (1954).

[74] J. Meng, Nucl. Phys. A **635**, 3 (1998).

[75] S.-G. Zhou, J. Meng, P. Ring, and E.-G. Zhao, Phys. Rev. C **82**, 011301(R) (2010).

[76] L. L. Li, J. Meng, P. Ring, E.-G. Zhao, and S.-G. Zhou, Phys. Rev. C **85**, 024312 (2012).

[77] Y. Chen, L. L. Li, H. Z. Liang, and J. Meng, Phys. Rev. C **85**, 067301 (2012).

[78] W. H. Long, H. Sagawa, J. Meng, and N. Van Giai, Europhys. Lett. **82**, 12001 (2008).

[79] L. J. Wang, J. M. Dong, and W. H. Long, Phys. Rev. **C 87**, 047301 (2013).

[80] L. J. Jiang, S. Yang, J. M. Dong, and W. H. Long, Phys. Rev. **C 91**, 025802 (2015).

[81] C. L. Bai, H. Sagawa, H. Q. Zhang, X. Z. Zhang, G. Colò, and F. R. Xu, Phys. Lett. B **675**, 28 (2009), ISSN 0370-2693,

[82] C. L. Bai, H. Q. Zhang, X. Z. Zhang, F. R. Xu, H. Sagawa, and G. Colò, Phys. Rev. C **79**, 041301(R) (2009),

[83] C. L. Bai, H. Q. Zhang, H. Sagawa, X. Z. Zhang, G. Colò, and F. R. Xu, Phys. Rev. Lett. **105**, 072501 (2010),

[84] C. L. Bai, H. Q. Zhang, H. Sagawa, X. Z. Zhang, G. Colò, and F. R. Xu, Phys. Rev. C **83**, 054316 (2011),

[85] C. L. Bai, H. Sagawa, G. Colò, H. Q. Zhang, and X. Z. Zhang, Phys. Rev. C **84**, 044329 (2011),

[86] W. H. Long, N. Van Giai, and J. Meng, Phys. Lett. **B 640**, 150 (2006).

[87] W. H. Long, H. Sagawa, N. Van Giai, and J. Meng, Phys. Rev. **C 76**, 034314 (2007).

[88] W. H. Long, T. Nakatsukasa, H. Sagawa, J. Meng, H. Nakada, and Y. Zhang, Phys. Lett. **B 680**, 428 (2009).

[89] J. J. Li, J. Margueron, W. H. Long, and N. V. Giai, Phys. Lett. B **753**, 97 (2016).

[90] L. J. Jiang, S. Yang, B. Y. Sun, W. H. Long, and H. Q. Gu, Phys. Rev. **C 91**, 034326 (2015).

[91] Y.-Y. Zong and B.-Y. Sun, Chin. Phys. C **42**, 024101 (2018).

[92] H. Z. Liang, N. Van Giai, and J. Meng, Phys. Rev. Lett. **101**, 122502 (2008).

[93] H. Z. Liang, N. Van Giai, and J. Meng, Phys. Rev. **C 79**, 064316 (2009).

[94] H. Z. Liang, P. W. Zhao, and J. Meng, Phys. Rev. **C 85**, 064302 (2012).

[95] Z. Niu, Y. Niu, H. Liang, W. Long, T. Nikšić, D. Vretenar, and J. Meng, Phys. Lett. **B 723**, 172 (2013).

[96] Z. M. Niu, Y. F. Niu, H. Z. Liang, W. H. Long, and J. Meng, Phys. Rev. C **95**, 044031 (2017).

[97] B. Y. Sun, W. H. Long, J. Meng, and U. Lombardo, Phys. Rev. **C 78**, 065805 (2008).

[98] W. H. Long, B. Y. Sun, K. Hagino, and H. Sagawa, Phys. Rev. **C 85**, 025806 (2012).

[99] Q. Zhao, B. Y. Sun, and W. H. Long, J. Phys. G: Nucl. Part. Phys. **42**, 095101 (2015).

[100] J. J. Li, W. H. Long, J. M. Margueron, and N. Van Giai, Phys. Lett. **B 732**, 169 (2014).

[101] J. J. Li, W. H. Long, J. Margueron, and N. V. Giai, Phys. Lett. B **788**, 192 (2019).

[102] W. H. Long, P. Ring, J. Meng, N. Van Giai, and C. A.

Bertulani, Phys. Rev. **C 81**, 031302(R) (2010).
[103] X. L. Lu, B. Y. Sun, and W. H. Long, Phys. Rev. **C 87**, 034311 (2013).
[104] J.-P. Ebran, E. Khan, D. Peña Arteaga, and D. Vretenar, Phys. Rev. **C 83**, 064323 (2011).
[105] J. Dobaczewski, W. Nazarewicz, T. R. Werner, J. F. Berger, C. R. Chinn, and J. Dechargé, Phys. Rev. C **53**, 2809 (1996).
[106] A. Bouyssy, J. F. Mathiot, N. V. Giai, and S. Marcos, Phys. Rev. **C 36**, 380 (1987).
[107] N. A. Lockerbie, A. V. Veryaskin, and X. Xu, J. Phys. A: Math. Gen. **29**, 4669 (1996).
[108] D. A. Varshalovich, A. N. Moskalev, and V. K. Khersonskii, Quantum Theory of Angular Momentum (World Scientific, Singapore, 1988).
[109] J. Meng and P. Ring, Phys. Rev. Lett. **77**, 3963 (1996).
[110] J. Meng, I. Tanihata, and S. Yamaji, Phys. Lett. B **419**, 1 (1998).
[111] J. Meng, Phys. Rev. C **57**, 1229 (1998).
[112] J. Meng and P. Ring, Phys. Rev. Lett. **80**, 460 (1998).
[113] J. F. Berger, M. Girod, and D. Gogny, Nucl. Phys. A **428**, 23 (1984).
[114] G. A. Lalazissis, T. Nikšić, D. Vretenar, and P. Ring, Phys. Rev. **C 71**, 024312 (2005).
[115] M. Wang, G. Audi, F. G. Kondev, W. J. Huang, S. Naimi, and X. Xu, Chinese Physics C **41** 030003 (2017).
[116] https://www.nndc.bnl.gov/nudat2/reCenter.jsp?z=26&n=30.
[117] https://www.nndc.bnl.gov/nudat2/reCenter.jsp?z=86&n=134.
[118] J. Xiang, Z. P. Li, J. M. Yao, W. H. Long, P. Ring, and J. Meng, Phys. Rev. C **88**, 057301 (2013).
[119] T. Otsuka, T. Suzuki, R. Fujimoto, H. Grawe, and Y. Akaishi, Phys. Rev. Lett. **95**, 232502 (2005).

Appendix A: Energy functionals and self-energies in various coupling channels

1. Compounded symbols

In the energy functionals, it is more convenient to express the expansion of the coupling strengths as

$$g_\phi(\rho_b) = \sqrt{2\pi}\sum_{\lambda_p} g_\phi^{\lambda_p}(r) Y_{\lambda_p 0}(\vartheta,\varphi), \tag{A1}$$

where g_ϕ corresponds to g_σ, g_ω, g_ρ, and f_π. In practice, we performed the integrations with respect to the angle variables $\mathbf{\Omega} = (\vartheta,\varphi)$ since the expansion of the wave functions $\psi_{\nu\pi m}$ is carried on the spherical Dirac Woods-Saxon (DWS) base $\psi_{n\kappa m}$. Such integration contains the Harmonic functions given by the expansions of the propagators (30), the coupling strengths (A1), and the couplings between the spherical spinors,

$$\sqrt{2\pi}\int d\mathbf{\Omega} Y_{\lambda_d\mu_d}(\mathbf{\Omega}) Y_{\lambda_y-\mu_y}(\mathbf{\Omega}) Y_{\lambda_p 0}(\mathbf{\Omega}) = \frac{1}{\sqrt{2}}\hat{\lambda}_d\hat{\lambda}_y\hat{\lambda}_p^{-1} C^{\lambda_p 0}_{\lambda_d 0\lambda_y 0} C^{\lambda_p 0}_{\lambda_d\mu\lambda_y-\mu}, \tag{A2}$$

where $\mu = \mu_d = \mu_y$, and (λ_d,μ_d), (λ_y,μ_y) and λ_p denote the terms due to the couplings between the spinors, the expansions of the propagators and the coupling strengths, respectively. As an abbreviation, we introduced the symbol Θ to denote the above integration,

$$\Theta^{\lambda_y\mu}_{\lambda_d\lambda_p} \equiv (-1)^\mu \frac{1}{\sqrt{2}}\hat{\lambda}_d\hat{\lambda}_y\hat{\lambda}_p^{-1} C^{\lambda_p 0}_{\lambda_d 0\lambda_y 0} C^{\lambda_p 0}_{\lambda_d\mu\lambda_y-\mu}. \tag{A3}$$

For the couplings between spherical spinors, we introduce the following symbols $\mathscr{D}$ ($\bar{\mathscr{D}}$) and $\mathcal{Q}$ ($\bar{\mathcal{Q}}$) as

$$\mathscr{D}^{\lambda\mu}_{\kappa_1 m_1;\kappa_2 m_2} = \frac{1}{\sqrt{2}}\hat{j}_1\hat{j}_2\hat{\lambda}^{-1} C^{L0}_{j_1\frac{1}{2}j_2-\frac{1}{2}} C^{\lambda\mu}_{j_1-m_1 j_2 m_2}, \tag{A4}$$

$$\bar{\mathscr{D}}^{\lambda\bar{\mu}}_{\kappa_1 m_1;\kappa_2 m_2} = (-1)^{\kappa_1}\mathscr{D}^{\lambda\bar{\mu}}_{\kappa_1-m_1;\kappa_2 m_2}, \tag{A5}$$

$$\mathcal{Q}^{\lambda\mu\sigma}_{\kappa_1 m_1;\kappa_2 m_2} \equiv (-1)^{j_1+l_1-\frac{1}{2}}\sqrt{3}\hat{j}_1\hat{j}_2\hat{l}_1\hat{l}_2 \sum_J C^{\lambda 0}_{l_1 0 l_2 0} C^{JM}_{\lambda\mu 1\sigma} \begin{Bmatrix} j_1 & j_2 & J \\ l_1 & l_2 & \lambda \\ \frac{1}{2} & \frac{1}{2} & 1 \end{Bmatrix} C^{JM}_{j_1-m_1 j_2 m_2}, \tag{A6}$$

$$\bar{\mathcal{Q}}^{\lambda\bar{\mu}\sigma}_{\kappa_1 m_1;\kappa_2 m_2} \equiv (-1)^{\kappa_1}\mathcal{Q}^{\lambda\bar{\mu}\sigma}_{\kappa_1-m_1;\kappa_2 m_2}. \tag{A7}$$

In the symbols $\mathscr{D}$ and $\bar{\mathscr{D}}$, $\mu = m_2 - m_1$ and $\bar{\mu} = m_2 + m_1$, and for $\mathcal{Q}$ and $\bar{\mathcal{Q}}$, one can find $\mu+\sigma = m_2 - m_1$ and $\bar{\mu}+\sigma = m_2 + m_1$. With these symbols, the couplings of the spherical spinors can be simply expressed as

$$\Omega^{l_1\dagger}_{j_1 m_1}\Omega^{l_2}_{j_2 m_2} = \frac{(-1)^{m_1+\frac{1}{2}}}{\sqrt{2\pi}}\sum_{\lambda_d}\mathscr{D}^{\lambda_d\mu_d}_{\kappa_1 m_1;\kappa_2 m_2} Y_{\lambda_d\mu_d}, \qquad \Omega^{l_1}_{j_1 m_1}\boldsymbol{\sigma}\Omega^{l_2}_{j_2 m_2} = \frac{(-1)^{m_1-\frac{1}{2}}}{\sqrt{2\pi}}\sum_{\lambda\mu\sigma}\mathcal{Q}^{\lambda_d\mu_d\sigma}_{\kappa_1 m_1;\kappa_2 m_2} Y_{\lambda_d\mu_d}\boldsymbol{e}_\sigma, \tag{A8}$$

where $\boldsymbol{e}_\sigma$ is the covariant spherical base vector with $\sigma = -1, 0, +1$. Notice that the quantity κ denotes the combination of the quantum numbers (j, l).

2. Energy functionals and self-energies from the Hartree terms

For σ-S coupling and the time component of ω-V one, the self-energies from the Hartree terms can be expressed as

$$\Sigma^{\lambda_d}_{S,\sigma}(r) = -2\pi \sum_{\lambda_p} g^{\lambda_p}_\sigma(r) \int r'^2 dr' \sum_{\lambda_y} \Theta^{\lambda_y 0}_{\lambda_d\lambda_p} R^\sigma_{\lambda_y\lambda_y}(r,r') \sum_{\lambda'_p\lambda'_d} \Theta^{\lambda_y 0}_{\lambda'_d\lambda'_p} g^{\lambda'_p}_\sigma(r')\rho^{\lambda'_d}_s(r'), \tag{A9a}$$

$$\Sigma^{\lambda_d}_{0,\omega}(r) = +2\pi \sum_{\lambda_p} g^{\lambda_p}_\omega(r) \int r'^2 dr' \sum_{\lambda_y} \Theta^{\lambda_y 0}_{\lambda_d\lambda_p} R^\omega_{\lambda_y\lambda_y}(r,r') \sum_{\lambda'_p\lambda'_d} \Theta^{\lambda_y 0}_{\lambda'_d\lambda'_p} g^{\lambda'_p}_\omega(r')\rho^{\lambda'_d}_b(r'). \tag{A9b}$$

Thus, the relevant energy functionals read as

$$E^D_\sigma = +\frac{2\pi}{2} \int r^2 dr \sum_{\lambda_d} \rho^{\lambda_d}_s(r)\Sigma^{\lambda_d}_{S,\sigma}(r), \qquad E^D_\omega = +\frac{2\pi}{2} \int r^2 dr \sum_{\lambda_d} \rho^{\lambda_d}_b(r)\Sigma^{\lambda_d}_{0,\omega}(r). \tag{A10a}$$

For the time component of ρ-V coupling, such expressions can be obtained by replacing $g^{\lambda_p}_\omega$ ($g^{\lambda'_p}_\omega$) with $g^{\lambda_p}_\rho$ ($g^{\lambda'_p}_\rho$) and $\rho^{\lambda_d}_b$ ($\rho^{\lambda'_d}_b$) with $\rho^{\lambda_d}_{b,3}$ ($\rho^{\lambda'_d}_{b,3}$), where $\rho^{\lambda_d}_{b,3} = \rho^{\lambda_d}_{b,n} - \rho^{\lambda_d}_{b,p}$. For the Coulomb field (A-V coupling), these expressions can be deduced by setting $\lambda_p = \lambda'_p = 0$ and replacing the nucleon density ρ_b as the proton one ρ_p. For the Hartree terms of the space components of the vector couplings, as well as the π-PV couplings, the contributions are derived as zero.

Since the coupling strengths g_σ, g_ω, and g_ρ are density-dependent, the variations of the energy functionals (A10) may lead to the additional rearrangement terms as

$$\Sigma^{D,\lambda_d}_{R,\sigma}(r) = -2\pi \sum_{\lambda_y} \sum_{\lambda_p\lambda_d} \Theta^{\lambda_y 0}_{\lambda_d\lambda_p} \left[\frac{\partial g^{\lambda_p}_\sigma}{\partial \rho^{\lambda_d}_b}\rho^{\lambda_d}_s\right]_r \int r'^2 dr' R^\sigma_{\lambda_y\lambda_y}(r,r') \sum_{\lambda'_p\lambda'_d} \Theta^{\lambda_y 0}_{\lambda'_d\lambda'_p} \left[g^{\lambda'_p}_\sigma \rho^{\lambda'_d}_s\right]_{r'}, \tag{A11}$$

$$\Sigma^{D,\lambda_d}_{R,\omega}(r) = +2\pi \sum_{\lambda_y} \sum_{\lambda_p\lambda_d} \Theta^{\lambda_y 0}_{\lambda_d\lambda_p} \left[\frac{\partial g^{\lambda_p}_\omega}{\partial \rho^{\lambda_d}_b}\rho^{\lambda_d}_b\right]_r \int r'^2 dr' R^\omega_{\lambda_y\lambda_y}(r,r') \sum_{\lambda'_p\lambda'_d} \Theta^{\lambda_y 0}_{\lambda'_d\lambda'_p} \left[g^{\lambda'_p}_\omega \rho^{\lambda'_d}_b\right]_{r'}. \tag{A12}$$

3. Energy functionals and self-energies from the Fock terms

For the Fock terms, the expressions are much more complicated than the Hartree terms. Notice that in deriving both the Hartree and Fock terms, we have set the angular momentum projection m to be positive for convenience. Thus, we need to revise the expansion of the spinor $\psi_{\nu\pi m}$. In principle, one can set the time conjugation partner as $\psi_{\nu\pi -m} \equiv \widehat{P}_t \psi_{\nu\pi m}$, $\widehat{P}_t$ being the time reversal operator, and the expansion of $\psi_{\nu\pi -m}$ reads as,

$$\psi_{\nu\pi -m} = \sum_\kappa (-1)^{j+l_u-m} \psi_{\nu\kappa -m}, \tag{A13}$$

where, by definition, $\psi_{\nu\kappa m}$ and $\psi_{\nu\kappa -m}$ share the radial components $\mathcal{G}_{i\kappa}$ and $\mathcal{F}_{i\kappa}$. For the Hartree terms, it does not bring additional complexity. While for the Fock terms, one has to carefully treat the couplings between the orbits m and $-m'$ ($m, m' > 0$). It can be found that the partner $(-m, -m')$ present identical contributions to the one (m, m'), and the partners $(m, -m')$ and $(-m, m')$ provide identical contributions.

To express the contributions of the Fock terms in compact form, we introduce the symbol $\widehat{\mathcal{D}}$ for σ-S coupling and

the time component of the vector ones as

$$\widehat{\mathcal{D}}^{\lambda_p\lambda'_p,\lambda_y;++}_{\kappa_1\kappa_2m;\kappa'_1\kappa'_2m'} = \frac{1}{2}\sum_{\lambda_d\lambda'_d}\left[\mathscr{D}^{\lambda_d\mu}_{\kappa_1m;\kappa'_1m'}\mathscr{D}^{\lambda'_d\mu}_{\kappa'_2m';\kappa_2m}\Theta^{\lambda_y\mu}_{\lambda_d\lambda_p}\Theta^{\lambda_y\mu}_{\lambda'_d\lambda'_p} + \bar{\mathscr{D}}^{\lambda_d\bar{\mu}}_{\kappa_1m;\kappa'_1m'}\bar{\mathscr{D}}^{\lambda'_d\bar{\mu}}_{\kappa'_2m';\kappa_2m}\Theta^{\lambda_y\bar{\mu}}_{\lambda_d\lambda_p}\Theta^{\lambda_y\bar{\mu}}_{\lambda'_d\lambda'_p}\right], \tag{A14}$$

$$\widehat{\mathcal{D}}^{\lambda_p\lambda'_p,\lambda_y;+-}_{\kappa_1\kappa_2m;\kappa'_1\kappa'_2m'} = \frac{1}{2}\sum_{\lambda_d\lambda'_d}\left[\mathscr{D}^{\lambda_d\mu}_{\kappa_1m;\kappa'_1m'}\mathscr{D}^{\lambda'_d\mu}_{-\kappa'_2m';-\kappa_2m}\Theta^{\lambda_y\mu}_{\lambda_d\lambda_p}\Theta^{\lambda_y\mu}_{\lambda'_d\lambda'_p} + \bar{\mathscr{D}}^{\lambda_d\bar{\mu}}_{\kappa_1m;\kappa'_1m'}\bar{\mathscr{D}}^{\lambda'_d\bar{\mu}}_{-\kappa'_2m';-\kappa_2m}\Theta^{\lambda_y\bar{\mu}}_{\lambda_d\lambda_p}\Theta^{\lambda_y\bar{\mu}}_{\lambda'_d\lambda'_p}\right], \tag{A15}$$

$$\widehat{\mathcal{D}}^{\lambda_p\lambda'_p,\lambda_y;-+}_{\kappa_1\kappa_2m;\kappa'_1\kappa'_2m'} = \frac{1}{2}\sum_{\lambda_d\lambda'_d}\left[\mathscr{D}^{\lambda_d\mu}_{-\kappa_1m;-\kappa'_1m'}\mathscr{D}^{\lambda'_d\mu}_{\kappa'_2m';\kappa_2m}\Theta^{\lambda_y\mu}_{\lambda_d\lambda_p}\Theta^{\lambda_y\mu}_{\lambda'_d\lambda'_p} + \bar{\mathscr{D}}^{\lambda_d\bar{\mu}}_{-\kappa_1m;-\kappa'_1m'}\bar{\mathscr{D}}^{\lambda'_d\bar{\mu}}_{\kappa'_2m';\kappa_2m}\Theta^{\lambda_y\bar{\mu}}_{\lambda_d\lambda_p}\Theta^{\lambda_y\bar{\mu}}_{\lambda'_d\lambda'_p}\right], \tag{A16}$$

$$\widehat{\mathcal{D}}^{\lambda_p\lambda'_p,\lambda_y;--}_{\kappa_1\kappa_2m;\kappa'_1\kappa'_2m'} = \frac{1}{2}\sum_{\lambda_d\lambda'_d}\left[\mathscr{D}^{\lambda_d\mu}_{-\kappa_1m;-\kappa'_1m'}\mathscr{D}^{\lambda'_d\mu}_{-\kappa'_2m';-\kappa_2m}\Theta^{\lambda_y\mu}_{\lambda_d\lambda_p}\Theta^{\lambda_y\mu}_{\lambda'_d\lambda'_p} + \bar{\mathscr{D}}^{\lambda_d\bar{\mu}}_{-\kappa_1m;-\kappa'_1m'}\bar{\mathscr{D}}^{\lambda'_d\bar{\mu}}_{-\kappa'_2m';-\kappa_2m}\Theta^{\lambda_y\bar{\mu}}_{\lambda_d\lambda_p}\Theta^{\lambda_y\bar{\mu}}_{\lambda'_d\lambda'_p}\right]. \tag{A17}$$

Notice that the terms contains $\mathscr{D}$ symbols correspond to the contributions from the partners (m,m') and $(-m,-m')$, and those containing the symbols $\bar{\mathscr{D}}$ for the partners $(m,-m')$ and $(-m,m')$. Thus, the nonlocal self-energies of the σ-S coupling can be expressed as

$$Y^{\kappa_1,\kappa_2;\sigma}_{G,\pi m} = +\frac{1}{2\pi}\sum_{\pi'm'}\delta_{\tau\tau'}\sum_{\kappa'_1\kappa'_2}\mathcal{R}^{++}_{\kappa'_1\kappa'_2,\pi'm'}(r,r')\sum_{\lambda_p\lambda'_p}g^{\lambda_p}_\sigma(r)g^{\lambda'_p}_\sigma(r')\sum_{\lambda_y}R^\sigma_{\lambda_y\lambda_y}(r,r')\widehat{\mathcal{D}}^{\lambda_p\lambda'_p,\lambda_y;++}_{\kappa'_1\kappa'_2m';\kappa_1\kappa_2m}, \tag{A18a}$$

$$Y^{\kappa_1,\kappa_2;\sigma}_{F,\pi m} = -\frac{1}{2\pi}\sum_{\pi'm'}\delta_{\tau\tau'}\sum_{\kappa'_1\kappa'_2}\mathcal{R}^{+-}_{\kappa'_1\kappa'_2,\pi'm'}(r,r')\sum_{\lambda_p\lambda'_p}g^{\lambda_p}_\sigma(r)g^{\lambda'_p}_\sigma(r')\sum_{\lambda_y}R^\sigma_{\lambda_y\lambda_y}(r,r')\widehat{\mathcal{D}}^{\lambda_p\lambda'_p,\lambda_y;+-}_{\kappa'_1\kappa'_2m';\kappa_1\kappa_2m}, \tag{A18b}$$

$$X^{\kappa_1,\kappa_2;\sigma}_{G,\pi m} = -\frac{1}{2\pi}\sum_{\pi'm'}\delta_{\tau\tau'}\sum_{\kappa'_1\kappa'_2}\mathcal{R}^{-+}_{\kappa'_1\kappa'_2,\pi'm'}(r,r')\sum_{\lambda_p\lambda'_p}g^{\lambda_p}_\sigma(r)g^{\lambda'_p}_\sigma(r')\sum_{\lambda_y}R^\sigma_{\lambda_y\lambda_y}(r,r')\widehat{\mathcal{D}}^{\lambda_p\lambda'_p,\lambda_y;-+}_{\kappa'_1\kappa'_2m';\kappa_1\kappa_2m}, \tag{A18c}$$

$$X^{\kappa_1,\kappa_2;\sigma}_{F,\pi m} = +\frac{1}{2\pi}\sum_{\pi'm'}\delta_{\tau\tau'}\sum_{\kappa'_1\kappa'_2}\mathcal{R}^{--}_{\kappa'_1\kappa'_2,\pi'm'}(r,r')\sum_{\lambda_p\lambda'_p}g^{\lambda_p}_\sigma(r)g^{\lambda'_p}_\sigma(r')\sum_{\lambda_y}R^\sigma_{\lambda_y\lambda_y}(r,r')\widehat{\mathcal{D}}^{\lambda_p\lambda'_p,\lambda_y;--}_{\kappa'_1\kappa'_2m';\kappa_1\kappa_2m}, \tag{A18d}$$

where the sum over ν' has been absorbed into the nonlocal densities $\mathcal{R}$, and the factor $\delta_{\tau\tau'}$ indicates that the orbits πm and $\pi' m'$ should be both neutron or proton ones. In terms of the nonlocal self-energies, the energy functional of the σ-S coupling reads as,

$$E^E_\sigma = \frac{1}{2}\int dr dr'\sum_i v_i^2\sum_{\kappa_1\kappa_2}\begin{pmatrix}\mathcal{G}_{i\kappa_1} & \mathcal{F}_{i\kappa_1}\end{pmatrix}_r\begin{pmatrix}Y^{\kappa_1,\kappa_2;\sigma}_{G,\pi m} & Y^{\kappa_1,\kappa_2;\sigma}_{F,\pi m}\\ X^{\kappa_1,\kappa_2;\sigma}_{G,\pi m} & X^{\kappa_1,\kappa_2;\sigma}_{F,\pi m}\end{pmatrix}_{r,r'}\begin{pmatrix}\mathcal{G}_{i\kappa_2}\\ \mathcal{F}_{i\kappa_2}\end{pmatrix}_{r'}, \tag{A19}$$

where v_i^2 ($\in[0,2]$) is the occupation number of the orbit $(\nu\pi m)$. For the rearrangement terms, the contribution to the self-energy $\Sigma_0^{\lambda_d}$ can be similarly expressed as

$$\Sigma^{E,\lambda_d}_{R,\sigma} = \int dr'\sum_i v_i^2\sum_{\kappa_1\kappa_2}\begin{pmatrix}\mathcal{G}_{i\kappa_1} & \mathcal{F}_{i\kappa_1}\end{pmatrix}_r\begin{pmatrix}P^{\kappa_1,\kappa_2;\sigma}_{G,\pi m,\lambda_d} & P^{\kappa_1,\kappa_2;\sigma}_{F,\pi m,\lambda_d}\\ Q^{\kappa_1,\kappa_2;\sigma}_{G,\pi m,\lambda_d} & Q^{\kappa_1,\kappa_2;\sigma}_{F,\pi m,\lambda_d}\end{pmatrix}_{r,r'}\begin{pmatrix}\mathcal{G}_{i\kappa_2}\\ \mathcal{F}_{i\kappa_2}\end{pmatrix}_{r'}, \tag{A20}$$

where the terms P and Q read as

$$P^{\kappa_1,\kappa_2;\sigma}_{G,\pi m,\lambda_d} = +\frac{1}{2\pi}\sum_{\pi'm'}\delta_{\tau\tau'}\sum_{\kappa'_1\kappa'_2}\mathcal{R}^{++}_{\kappa'_1\kappa'_2,\pi'm'}(r,r')\sum_{\lambda_p\lambda'_p}\frac{\partial g^{\lambda_p}_\sigma(r)}{\partial\rho^{\lambda_d}_b(r)}g^{\lambda'_p}_\sigma(r')\sum_{\lambda_y}R^\sigma_{\lambda_y\lambda_y}(r,r')\widehat{\mathcal{D}}^{\lambda_p\lambda'_p,\lambda_y;++}_{\kappa'_1\kappa'_2m';\kappa_1\kappa_2m}, \tag{A21a}$$

$$P^{\kappa_1,\kappa_2;\sigma}_{F,\pi m,\lambda_d} = -\frac{1}{2\pi}\sum_{\pi'm'}\delta_{\tau\tau'}\sum_{\kappa'_1\kappa'_2}\mathcal{R}^{+-}_{\kappa'_1\kappa'_2,\pi'm'}(r,r')\sum_{\lambda_p\lambda'_p}\frac{\partial g^{\lambda_p}_\sigma(r)}{\partial\rho^{\lambda_d}_b(r)}g^{\lambda'_p}_\sigma(r')\sum_{\lambda_y}R^\sigma_{\lambda_y\lambda_y}(r,r')\widehat{\mathcal{D}}^{\lambda_p\lambda'_p,\lambda_y;+-}_{\kappa'_1\kappa'_2m';\kappa_1\kappa_2m}, \tag{A21b}$$

$$Q^{\kappa_1,\kappa_2;\sigma}_{G,\pi m,\lambda_d} = -\frac{1}{2\pi}\sum_{\pi'm'}\delta_{\tau\tau'}\sum_{\kappa'_1\kappa'_2}\mathcal{R}^{-+}_{\kappa'_1\kappa'_2,\pi'm'}(r,r')\sum_{\lambda_p\lambda'_p}\frac{\partial g^{\lambda_p}_\sigma(r)}{\partial\rho^{\lambda_d}_b(r)}g^{\lambda'_p}_\sigma(r')\sum_{\lambda_y}R^\sigma_{\lambda_y\lambda_y}(r,r')\widehat{\mathcal{D}}^{\lambda_p\lambda'_p,\lambda_y;-+}_{\kappa'_1\kappa'_2m';\kappa_1\kappa_2m}, \tag{A21c}$$

$$Q^{\kappa_1,\kappa_2;\sigma}_{F,\pi m,\lambda_d} = +\frac{1}{2\pi}\sum_{\pi'm'}\delta_{\tau\tau'}\sum_{\kappa'_1\kappa'_2}\mathcal{R}^{--}_{\kappa'_1\kappa'_2,\pi'm'}(r,r')\sum_{\lambda_p\lambda'_p}\frac{\partial g^{\lambda_p}_\sigma(r)}{\partial\rho^{\lambda_d}_b(r)}g^{\lambda'_p}_\sigma(r')\sum_{\lambda_y}R^\sigma_{\lambda_y\lambda_y}(r,r')\widehat{\mathcal{D}}^{\lambda_p\lambda'_p,\lambda_y;--}_{\kappa'_1\kappa'_2m';\kappa_1\kappa_2m}. \tag{A21d}$$

For the time components of the vector couplings, similar expressions can be obtained by replacing the expansion terms of the propagator $R^{\sigma}_{\lambda_y\lambda_y}$ and the coupling strengths $g^{\lambda_p}_{\sigma}$ in Eqs. (A18), (A21) with the corresponding ones, and additionally the plus signs in the Y_G, X_F, P_G and Q_F terms should be changed as the minus one. It should be also noticed that for the isovector ρ-V coupling, the factor $\delta_{\tau\tau'}$ shall be replaced by $(2-\delta_{\tau\tau'})$. For the Fock terms of the Coulomb interaction, there is no arrangement term and for the non-local self-energies [see Eqs. (A18)] only $\lambda_p=\lambda'_p=0$ terms remain.

For the space component of the vector couplings, we take the ω-V coupling as examples, and the others can be similarly deduced. To write the expressions in a compact form, we introduce the symbols $\widehat{\mathcal{B}}$ as

$$\widehat{\mathcal{B}}^{\lambda_p\lambda'_p,\lambda_y;++}_{\kappa'_1\kappa'_2m';\kappa_1\kappa_2m}\equiv\frac{1}{2}\sum_{\lambda_d\lambda'_d\sigma}\left[\mathcal{Q}^{\lambda_d\mu\sigma}_{-\kappa'_1m',\kappa_1m}\mathcal{Q}^{\lambda'_d\mu\sigma}_{-\kappa'_2m',\kappa_2m}\Theta^{\lambda_y\mu}_{\lambda_d\lambda_p}\Theta^{\lambda_y\mu}_{\lambda'_d\lambda'_p}+\bar{\mathcal{Q}}^{\lambda_d\bar{\mu}\sigma}_{-\kappa'_1m',\kappa_1m}\bar{\mathcal{Q}}^{\lambda'_d\bar{\mu}\sigma}_{-\kappa'_2m',\kappa_2m}\Theta^{\lambda_y\bar{\mu}}_{\lambda_d\lambda_p}\Theta^{\lambda_y\bar{\mu}}_{\lambda'_d\lambda'_p}\right], \tag{A22}$$

$$\widehat{\mathcal{B}}^{\lambda_p\lambda'_p,\lambda_y;+-}_{\kappa'_1\kappa'_2m';\kappa_1\kappa_2m}\equiv\frac{1}{2}\sum_{\lambda_d\lambda'_d\sigma}\left[\mathcal{Q}^{\lambda_d\mu\sigma}_{-\kappa'_1m',\kappa_1m}\mathcal{Q}^{\lambda'_d\mu\sigma}_{\kappa'_2m',-\kappa_2m}\Theta^{\lambda_y\mu}_{\lambda_d\lambda_p}\Theta^{\lambda_y\mu}_{\lambda'_d\lambda'_p}+\bar{\mathcal{Q}}^{\lambda_d\bar{\mu}\sigma}_{-\kappa'_1m',\kappa_1m}\bar{\mathcal{Q}}^{\lambda'_d\bar{\mu}\sigma}_{\kappa'_2m',-\kappa_2m}\Theta^{\lambda_y\bar{\mu}}_{\lambda_d\lambda_p}\Theta^{\lambda_y\bar{\mu}}_{\lambda'_d\lambda'_p}\right], \tag{A23}$$

$$\widehat{\mathcal{B}}^{\lambda_p\lambda'_p,\lambda_y;-+}_{\kappa'_1\kappa'_2m';\kappa_1\kappa_2m}\equiv\frac{1}{2}\sum_{\lambda_d\lambda'_d\sigma}\left[\mathcal{Q}^{\lambda_d\mu\sigma}_{\kappa'_1m',-\kappa_1m}\mathcal{Q}^{\lambda'_d\mu\sigma}_{-\kappa'_2m',\kappa_2m}\Theta^{\lambda_y\mu}_{\lambda_d\lambda_p}\Theta^{\lambda_y\mu}_{\lambda'_d\lambda'_p}+\bar{\mathcal{Q}}^{\lambda_d\bar{\mu}\sigma}_{\kappa'_1m',-\kappa_1m}\bar{\mathcal{Q}}^{\lambda'_d\bar{\mu}\sigma}_{-\kappa'_2m',\kappa_2m}\Theta^{\lambda_y\bar{\mu}}_{\lambda_d\lambda_p}\Theta^{\lambda_y\bar{\mu}}_{\lambda'_d\lambda'_p}\right], \tag{A24}$$

$$\widehat{\mathcal{B}}^{\lambda_p\lambda'_p,\lambda_y;--}_{\kappa'_1\kappa'_2m';\kappa_1\kappa_2m}\equiv\frac{1}{2}\sum_{\lambda_d\lambda'_d\sigma}\left[\mathcal{Q}^{\lambda_d\mu\sigma}_{\kappa'_1m',-\kappa_1m}\mathcal{Q}^{\lambda'_d\mu\sigma}_{\kappa'_2m',-\kappa_2m}\Theta^{\lambda_y\mu}_{\lambda_d\lambda_p}\Theta^{\lambda_y\mu}_{\lambda'_d\lambda'_p}+\bar{\mathcal{Q}}^{\lambda_d\bar{\mu}\sigma}_{\kappa'_1m',-\kappa_1m}\bar{\mathcal{Q}}^{\lambda'_d\bar{\mu}\sigma}_{\kappa'_2m',-\kappa_2m}\Theta^{\lambda_y\bar{\mu}}_{\lambda_d\lambda_p}\Theta^{\lambda_y\bar{\mu}}_{\lambda'_d\lambda'_p}\right]. \tag{A25}$$

Thus, the nonlocal self-energies can be expressed as

$$Y^{\kappa_1,\kappa_2;\boldsymbol{\omega}}_{G,\pi m}=+\frac{1}{2\pi}\sum_{\pi'm'}\delta_{\tau\tau'}\sum_{\kappa'_1\kappa'_2}\mathcal{R}^{--}_{\kappa'_1\kappa'_2,\pi'm'}(r,r')\sum_{\lambda_p\lambda'_p}g^{\lambda_p}_{\omega}(r)g^{\lambda'_p}_{\omega}(r')\sum_{\lambda_y}R^{\omega}_{\lambda_y\lambda_y}(r,r')\widehat{\mathcal{B}}^{\lambda_p\lambda'_p,\lambda_y;++}_{\kappa'_1\kappa'_2m';\kappa_1\kappa_2m}, \tag{A26}$$

$$Y^{\kappa_1,\kappa_2;\boldsymbol{\omega}}_{F,\pi m}=-\frac{1}{2\pi}\sum_{\pi'm'}\delta_{\tau\tau'}\sum_{\kappa'_1\kappa'_2}\mathcal{R}^{-+}_{\kappa'_1\kappa'_2,\pi'm'}(r,r')\sum_{\lambda_p\lambda'_p}g^{\lambda_p}_{\omega}(r)g^{\lambda'_p}_{\omega}(r')\sum_{\lambda_y}R^{\omega}_{\lambda_y\lambda_y}(r,r')\widehat{\mathcal{B}}^{\lambda_p\lambda'_p,\lambda_y;+-}_{\kappa'_1\kappa'_2m';\kappa_1\kappa_2m}, \tag{A27}$$

$$X^{\kappa_1,\kappa_2;\boldsymbol{\omega}}_{G,\pi m}=-\frac{1}{2\pi}\sum_{\pi'm'}\delta_{\tau\tau'}\sum_{\kappa'_1\kappa'_2}\mathcal{R}^{+-}_{\kappa'_1\kappa'_2,\pi'm'}(r,r')\sum_{\lambda_p\lambda'_p}g^{\lambda_p}_{\omega}(r)g^{\lambda'_p}_{\omega}(r')\sum_{\lambda_y}R^{\omega}_{\lambda_y\lambda_y}(r,r')\widehat{\mathcal{B}}^{\lambda_p\lambda'_p,\lambda_y;-+}_{\kappa'_1\kappa'_2m';\kappa_1\kappa_2m}, \tag{A28}$$

$$X^{\kappa_1,\kappa_2;\boldsymbol{\omega}}_{F,\pi m}=+\frac{1}{2\pi}\sum_{\pi'm'}\delta_{\tau\tau'}\sum_{\kappa'_1\kappa'_2}\mathcal{R}^{++}_{\kappa'_1\kappa'_2,\pi'm'}(r,r')\sum_{\lambda_p\lambda'_p}g^{\lambda_p}_{\omega}(r)g^{\lambda'_p}_{\omega}(r')\sum_{\lambda_y}R^{\omega}_{\lambda_y\lambda_y}(r,r')\widehat{\mathcal{B}}^{\lambda_p\lambda'_p,\lambda_y;--}_{\kappa'_1\kappa'_2m';\kappa_1\kappa_2m}. \tag{A29}$$

Here, we use the bold type $\boldsymbol{\omega}$ to represent the space component. In terms of the above nonlocal self-energies, the energy functional from the space component of the ω-V coupling reads as

$$E^{E}_{\boldsymbol{\omega}}=\frac{1}{2}\int drdr'\sum_i v_i^2\sum_{\kappa_1\kappa_2}\begin{pmatrix}\mathcal{G}_{i\kappa_1} & \mathcal{F}_{i\kappa_1}\end{pmatrix}_r\begin{pmatrix}Y^{\kappa_1,\kappa_2;\boldsymbol{\omega}}_{G,\pi m} & Y^{\kappa_1,\kappa_2;\boldsymbol{\omega}}_{F,\pi m}\\ X^{\kappa_1,\kappa_2;\boldsymbol{\omega}}_{G,\pi m} & X^{\kappa_1,\kappa_2;\boldsymbol{\omega}}_{F,\pi m}\end{pmatrix}_{r,r'}\begin{pmatrix}\mathcal{G}_{i\kappa_2}\\ \mathcal{F}_{i\kappa_2}\end{pmatrix}_{r'}. \tag{A30}$$

For the rearrangement terms, the contribution to the self-energy can be similarly expressed as

$$\Sigma^{E,\lambda_d}_{R,\boldsymbol{\omega}}=\int dr'\sum_i v_i^2\sum_{\kappa_1\kappa_2}\begin{pmatrix}\mathcal{G}_{i\kappa_1} & \mathcal{F}_{i\kappa_1}\end{pmatrix}_r\begin{pmatrix}P^{\kappa_1,\kappa_2;\boldsymbol{\omega}}_{G,\pi m,\lambda_d} & P^{\kappa_1,\kappa_2;\boldsymbol{\omega}}_{F,\pi m,\lambda_d}\\ Q^{\kappa_1,\kappa_2;\boldsymbol{\omega}}_{G,\pi m,\lambda_d} & Q^{\kappa_1,\kappa_2;\boldsymbol{\omega}}_{F,\pi m,\lambda_d}\end{pmatrix}_{r,r'}\begin{pmatrix}\mathcal{G}_{i\kappa_2}\\ \mathcal{F}_{i\kappa_2}\end{pmatrix}_{r'}, \tag{A31}$$

where the P and Q terms read as

$$P^{\kappa_1,\kappa_2;\boldsymbol{\omega}}_{G,\pi m,\lambda_d}=+\frac{1}{2\pi}\sum_{\pi'm'}\delta_{\tau\tau'}\sum_{\kappa'_1\kappa'_2}\mathcal{R}^{--}_{\kappa'_1\kappa'_2,\pi'm'}(r,r')\sum_{\lambda_p\lambda'_p}\frac{\partial g^{\lambda_p}_{\omega}(r)}{\partial\rho^{\lambda_d}_b(r)}g^{\lambda'_p}_{\omega}(r')\sum_{\lambda_y}R^{\omega}_{\lambda_y\lambda_y}(r,r')\widehat{\mathcal{B}}^{\lambda_p\lambda'_p,\lambda_y;++}_{\kappa'_1\kappa'_2m';\kappa_1\kappa_2m}, \tag{A32}$$

$$P^{\kappa_1,\kappa_2;\boldsymbol{\omega}}_{F,\pi m,\lambda_d}=-\frac{1}{2\pi}\sum_{\pi'm'}\delta_{\tau\tau'}\sum_{\kappa'_1\kappa'_2}\mathcal{R}^{-+}_{\kappa'_1\kappa'_2,\pi'm'}(r,r')\sum_{\lambda_p\lambda'_p}\frac{\partial g^{\lambda_p}_{\omega}(r)}{\partial\rho^{\lambda_d}_b(r)}g^{\lambda'_p}_{\omega}(r')\sum_{\lambda_y}R^{\omega}_{\lambda_y\lambda_y}(r,r')\widehat{\mathcal{B}}^{\lambda_p\lambda'_p,\lambda_y;+-}_{\kappa'_1\kappa'_2m';\kappa_1\kappa_2m}, \tag{A33}$$

$$Q^{\kappa_1,\kappa_2;\boldsymbol{\omega}}_{G,\pi m,\lambda_d}=-\frac{1}{2\pi}\sum_{\pi'm'}\delta_{\tau\tau'}\sum_{\kappa'_1\kappa'_2}\mathcal{R}^{+-}_{\kappa'_1\kappa'_2,\pi'm'}(r,r')\sum_{\lambda_p\lambda'_p}\frac{\partial g^{\lambda_p}_{\omega}(r)}{\partial\rho^{\lambda_d}_b(r)}g^{\lambda'_p}_{\omega}(r')\sum_{\lambda_y}R^{\omega}_{\lambda_y\lambda_y}(r,r')\widehat{\mathcal{B}}^{\lambda_p\lambda'_p,\lambda_y;-+}_{\kappa'_1\kappa'_2m';\kappa_1\kappa_2m}, \tag{A34}$$

$$Q^{\kappa_1,\kappa_2;\boldsymbol{\omega}}_{F,\pi m,\lambda_d}=+\frac{1}{2\pi}\sum_{\pi'm'}\delta_{\tau\tau'}\sum_{\kappa'_1\kappa'_2}\mathcal{R}^{++}_{\kappa'_1\kappa'_2,\pi'm'}(r,r')\sum_{\lambda_p\lambda'_p}\frac{\partial g^{\lambda_p}_{\omega}(r)}{\partial\rho^{\lambda_d}_b(r)}g^{\lambda'_p}_{\omega}(r')\sum_{\lambda_y}R^{\omega}_{\lambda_y\lambda_y}(r,r')\widehat{\mathcal{B}}^{\lambda_p\lambda'_p,\lambda_y;--}_{\kappa'_1\kappa'_2m';\kappa_1\kappa_2m}. \tag{A35}$$

For the other vector couplings, the expressions can be obtained by replacing the expansion terms of the propagator and coupling strengths with the relevant ones. In addition, for the isovector ρ-V coupling, one needs to replace the isospin factor $\delta_{\tau\tau'}$ by $(2-\delta_{\tau\tau'})$, and for the Coulomb interaction only the $\lambda_p=\lambda'_p=0$ terms remain.

For the π-PV coupling, the situation becomes even more complicated. First there exist gradient operations over the propagator, which can be expressed as

$$\begin{aligned}\boldsymbol{\nabla}_{\boldsymbol{r}}\boldsymbol{\nabla}_{\boldsymbol{r}'}D_\pi(\boldsymbol{r},\boldsymbol{r}') =& m_\pi^2\sum_{L=0}^{\infty}\sum_{\lambda_y\lambda'_y}^{L\pm1}C_{L010}^{\lambda_y 0}C_{L010}^{\lambda'_y 0}\mathcal{V}_L^{\lambda_y\lambda'_y}(m_\pi,r,r')\\ &\times\sum_M(-1)^M\sum_{\mu_y\sigma_y}C^{LM}_{\lambda_y\mu_y1\sigma_y}Y_{\lambda_y\mu_y}(\vartheta,\varphi)\boldsymbol{e}_{\sigma_y}\sum_{\mu'_y\sigma'_y}C^{LM}_{\lambda'_y\mu'_y1\sigma'_y}Y_{\lambda'_y-\mu'_y}(\vartheta',\varphi')\boldsymbol{e}_{-\sigma'_y},\end{aligned}\tag{A36}$$

where the radial terms read as

$$\mathcal{V}_L^{\lambda_y\lambda'_y}(m_\pi;r,r')\equiv -R_{\lambda_y\lambda'_y}(m_\pi;r,r')+\frac{1}{m_\pi^2r^2}\delta(r-r').\tag{A37}$$

To have compact expressions, we introduce the symbols $\mathcal{P}$ and $\bar{\mathcal{P}}$ as

$$\sum_{\lambda_d}C_{L010}^{\lambda_y0}C^{L\mathcal{M}}_{\lambda_y\mu1\sigma}\mathcal{Q}^{\lambda_d\mu\sigma}_{\kappa'_1m',\kappa_1m}\Theta^{\lambda_y\mu}_{\lambda_d\lambda_p}\equiv\mathcal{P}^{\lambda_p,L\lambda_y;\mu\sigma}_{\kappa'_1m',\kappa_1m},\qquad \sum_{\lambda_d}C_{L010}^{\lambda_y0}C^{L\mathcal{M}}_{\lambda_y\mu1\sigma}\bar{\mathcal{Q}}^{\lambda_d\mu\sigma}_{\kappa'_1m',\kappa_1m}\Theta^{\lambda_y\mu}_{\lambda_d\lambda_p}\equiv\bar{\mathcal{P}}^{\lambda_p,L\lambda_y;\bar{\mu}\sigma}_{\kappa'_1m',\kappa_1m},\tag{A38}$$

and further the symbols $\widehat{\mathcal{A}}$ for the combinations of $\mathcal{P}$ and $\bar{\mathcal{P}}$ as

$$\widehat{\mathcal{A}}^{\lambda_p\lambda'_p,L\lambda_y\lambda'_y;++}_{\kappa'_1\kappa'_2m';\kappa_1\kappa_2m}\equiv\frac{1}{2}\left\{\sum_{\sigma\sigma'}\mathcal{P}^{\lambda_p,L\lambda_y;\mu\sigma}_{\kappa'_1m',\kappa_1m}\mathcal{P}^{\lambda'_p,L\lambda'_y;\mu'\sigma'}_{\kappa'_2m',\kappa_2m}+\sum_{\sigma\sigma'}\bar{\mathcal{P}}^{\lambda_p,L\lambda_y;\bar{\mu}\sigma}_{\kappa'_1m',\kappa_1m}\bar{\mathcal{P}}^{\lambda'_p,L\lambda'_y;\bar{\mu}'\sigma'}_{\kappa'_2m',\kappa_2m}\right\},\tag{A39a}$$

$$\widehat{\mathcal{A}}^{\lambda_p\lambda'_p,L\lambda_y\lambda'_y;+-}_{\kappa'_1\kappa'_2m';\kappa_1\kappa_2m}\equiv\frac{1}{2}\left\{\sum_{\sigma\sigma'}\mathcal{P}^{\lambda_p,L\lambda_y;\mu\sigma}_{\kappa'_1m',\kappa_1m}\mathcal{P}^{\lambda'_p,L\lambda'_y;\mu'\sigma'}_{-\kappa'_2m',-\kappa_2m}+\sum_{\sigma\sigma'}\bar{\mathcal{P}}^{\lambda_p,L\lambda_y;\bar{\mu}\sigma}_{\kappa'_1m',\kappa_1m}\bar{\mathcal{P}}^{\lambda'_p,L\lambda'_y;\bar{\mu}'\sigma'}_{-\kappa'_2m',-\kappa_2m}\right\},\tag{A39b}$$

$$\widehat{\mathcal{A}}^{\lambda_p\lambda'_p,L\lambda_y\lambda'_y;-+}_{\kappa'_1\kappa'_2m';\kappa_1\kappa_2m}\equiv\frac{1}{2}\left\{\sum_{\sigma\sigma'}\mathcal{P}^{\lambda_p,L\lambda_y;\mu\sigma}_{-\kappa'_1m',-\kappa_1m}\mathcal{P}^{\lambda'_p,L\lambda'_y;\mu'\sigma'}_{\kappa'_2m',\kappa_2m}+\sum_{\sigma\sigma'}\bar{\mathcal{P}}^{\lambda_p,L\lambda_y;\bar{\mu}\sigma}_{-\kappa'_1m',-\kappa_1m}\bar{\mathcal{P}}^{\lambda'_p,L\lambda'_y;\bar{\mu}'\sigma'}_{\kappa'_2m',\kappa_2m}\right\},\tag{A39c}$$

$$\widehat{\mathcal{A}}^{\lambda_p\lambda'_p,L\lambda_y\lambda'_y;--}_{\kappa'_1\kappa'_2m';\kappa_1\kappa_2m}\equiv\frac{1}{2}\left\{\sum_{\sigma\sigma'}\mathcal{P}^{\lambda_p,L\lambda_y;\mu\sigma}_{-\kappa'_1m',-\kappa_1m}\mathcal{P}^{\lambda'_p,L\lambda'_y;\mu'\sigma'}_{-\kappa'_2m',-\kappa_2m}+\sum_{\sigma\sigma'}\bar{\mathcal{P}}^{\lambda_p,L\lambda_y;\bar{\mu}\sigma}_{-\kappa'_1m',-\kappa_1m}\bar{\mathcal{P}}^{\lambda'_p,L\lambda'_y;\bar{\mu}'\sigma'}_{-\kappa'_2m',-\kappa_2m}\right\},\tag{A39d}$$

where $\mu+\sigma=\mu'+\sigma'=m-m'$ and $\bar{\mu}+\sigma=\bar{\mu}'+\sigma'=m+m'$. With the defined symbols, the self-energies from the π-PV coupling can be expressed as

$$Y^{\kappa_1\kappa_2,\pi}_{G,\pi m}=\frac{1}{2\pi}\sum_{\pi'm'}(2-\delta_{\tau\tau'})\sum_{\kappa'_1\kappa'_2}\mathcal{R}^{++}_{\kappa'_1\kappa'_2,\pi'm'}(r,r')\sum_{\lambda_p\lambda'_p}f_\pi^{\lambda_p}(r)f_\pi^{\lambda'_p}(r')\sum_L\sum_{\lambda_y\lambda'_y}^{L\pm1}\mathcal{V}_L^{\lambda_y\lambda'_y}(r,r')\widehat{\mathcal{A}}^{\lambda_p\lambda'_p,L\lambda_y\lambda'_y;++}_{\kappa'_1\kappa'_2m';\kappa_1\kappa_2m};\tag{A40}$$

$$Y^{\kappa_1\kappa_2,\pi}_{F,\pi m}=\frac{1}{2\pi}\sum_{\pi'm'}(2-\delta_{\tau\tau'})\sum_{\kappa'_1\kappa'_2}\mathcal{R}^{+-}_{\kappa'_1\kappa'_2,\pi'm'}(r,r')\sum_{\lambda_p\lambda'_p}f_\pi^{\lambda_p}(r)f_\pi^{\lambda'_p}(r')\sum_L\sum_{\lambda_y\lambda'_y}^{L\pm1}\mathcal{V}_L^{\lambda_y\lambda'_y}(r,r')\widehat{\mathcal{A}}^{\lambda_p\lambda'_p,L\lambda_y\lambda'_y;+-}_{\kappa'_1\kappa'_2m';\kappa_1\kappa_2m};\tag{A41}$$

$$X^{\kappa_1\kappa_2,\pi}_{G,\pi m}=\frac{1}{2\pi}\sum_{\pi'm'}(2-\delta_{\tau\tau'})\sum_{\kappa'_1\kappa'_2}\mathcal{R}^{-+}_{\kappa'_1\kappa'_2,\pi'm'}(r,r')\sum_{\lambda_p\lambda'_p}f_\pi^{\lambda_p}(r)f_\pi^{\lambda'_p}(r')\sum_L\sum_{\lambda_y\lambda'_y}^{L\pm1}\mathcal{V}_L^{\lambda_y\lambda'_y}(r,r')\widehat{\mathcal{A}}^{\lambda_p\lambda'_p,L\lambda_y\lambda'_y;-+}_{\kappa'_1\kappa'_2m';\kappa_1\kappa_2m};\tag{A42}$$

$$X^{\kappa_1\kappa_2,\pi}_{F,\pi m}=\frac{1}{2\pi}\sum_{\pi'm'}(2-\delta_{\tau\tau'})\sum_{\kappa'_1\kappa'_2}\mathcal{R}^{--}_{\kappa'_1\kappa'_2,\pi'm'}(r,r')\sum_{\lambda_p\lambda'_p}f_\pi^{\lambda_p}(r)f_\pi^{\lambda'_p}(r')\sum_L\sum_{\lambda_y\lambda'_y}^{L\pm1}\mathcal{V}_L^{\lambda_y\lambda'_y}(r,r')\widehat{\mathcal{A}}^{\lambda_p\lambda'_p,L\lambda_y\lambda'_y;--}_{\kappa'_1\kappa'_2m';\kappa_1\kappa_2m}.\tag{A43}$$

In terms of the non-local self-energies, the energy functional from the π-PV coupling reads as

$$E^E_{\pi-\mathrm{PV}}=\frac{1}{2}\int drdr'\sum_i v_i^2\sum_{\kappa_1\kappa_2}\begin{pmatrix}\mathcal{G}_{i\kappa_1}(r) & \mathcal{F}_{i\kappa_1}(r)\end{pmatrix}\begin{pmatrix}Y^{\kappa_1\kappa_2,\pi}_{G,\pi m} & Y^{\kappa_1\kappa_2,\pi}_{F,\pi m}\\ X^{\kappa_1\kappa_2,\pi}_{G,\pi m} & X^{\kappa_1\kappa_2,\pi}_{F,\pi m}\end{pmatrix}_{r,r'}\begin{pmatrix}\mathcal{G}_{i\kappa_2}(r')\\ \mathcal{F}_{i\kappa_2}(r')\end{pmatrix}.\tag{A44}$$

Similarly the rearrangement term $\Sigma_{R,\pi}^{E,\lambda_d}$ can be expressed as

$$\Sigma_{R,\pi}^{E,\lambda_d} = \int dr' \sum_i v_i^2 \sum_{\kappa_1\kappa_2} \begin{pmatrix} \mathcal{G}_{i\kappa_1}(r) & \mathcal{F}_{i\kappa_1}(r) \end{pmatrix} \begin{pmatrix} P_{G,\pi m,\lambda_d}^{\kappa_a\kappa_b,\pi} & P_{F,\pi m,\lambda_d}^{\kappa_a\kappa_b,\pi} \\ Q_{G,\pi m,\lambda_d}^{\kappa_a\kappa_b,\pi} & Q_{F,\pi m,\lambda_d}^{\kappa_a\kappa_b,\pi} \end{pmatrix}_{r,r'} \begin{pmatrix} \mathcal{G}_{i\kappa_2}(r') \\ \mathcal{F}_{i\kappa_2}(r') \end{pmatrix}, \tag{A45}$$

where the terms P and Q read as

$$P_{G,\pi m,\lambda_d}^{\kappa_1\kappa_2,\pi} = \frac{1}{2\pi} \sum_{\pi' m'} (2-\delta_{\tau\tau'}) \sum_{\kappa_1'\kappa_2'} \mathcal{R}_{\kappa_1'\kappa_2',\pi' m'}^{++}(r,r') \sum_{\lambda_p\lambda_p'} \frac{\partial f_\pi^{\lambda_p}(r)}{\partial \rho_b^{\lambda_d}(r)} f_\pi^{\lambda_p'}(r') \sum_L \sum_{\lambda_y\lambda_y'}^{L\pm1} \mathcal{V}_L^{\lambda_y\lambda_y'}(r,r') \widehat{\mathcal{A}}_{\kappa_1'\kappa_2' m';\kappa_1\kappa_2 m}^{\lambda_p\lambda_p',L\lambda_y\lambda_y';++}; \tag{A46}$$

$$P_{F,\pi m,\lambda_d}^{\kappa_1\kappa_2,\pi} = \frac{1}{2\pi} \sum_{\pi' m'} (2-\delta_{\tau\tau'}) \sum_{\kappa_1'\kappa_2'} \mathcal{R}_{\kappa_1'\kappa_2',\pi' m'}^{+-}(r,r') \sum_{\lambda_p\lambda_p'} \frac{\partial f_\pi^{\lambda_p}(r)}{\partial \rho_b^{\lambda_d}(r)} f_\pi^{\lambda_p'}(r') \sum_L \sum_{\lambda_y\lambda_y'}^{L\pm1} \mathcal{V}_L^{\lambda_y\lambda_y'}(r,r') \widehat{\mathcal{A}}_{\kappa_1'\kappa_2' m';\kappa_1\kappa_2 m}^{\lambda_p\lambda_p',L\lambda_y\lambda_y';+-}; \tag{A47}$$

$$Q_{G,\pi m,\lambda_d}^{\kappa_1\kappa_2,\pi} = \frac{1}{2\pi} \sum_{\pi' m'} (2-\delta_{\tau\tau'}) \sum_{\kappa_1'\kappa_2'} \mathcal{R}_{\kappa_1'\kappa_2',\pi' m'}^{-+}(r,r') \sum_{\lambda_p\lambda_p'} \frac{\partial f_\pi^{\lambda_p}(r)}{\partial \rho_b^{\lambda_d}(r)} f_\pi^{\lambda_p'}(r') \sum_L \sum_{\lambda_y\lambda_y'}^{L\pm1} \mathcal{V}_L^{\lambda_y\lambda_y'}(r,r') \widehat{\mathcal{A}}_{\kappa_1'\kappa_2' m';\kappa_1\kappa_2 m}^{\lambda_p\lambda_p',L\lambda_y\lambda_y';-+}; \tag{A48}$$

$$Q_{F,\pi m,\lambda_d}^{\kappa_1\kappa_2,\pi} = \frac{1}{2\pi} \sum_{\pi' m'} (2-\delta_{\tau\tau'}) \sum_{\kappa_1'\kappa_2'} \mathcal{R}_{\kappa_1'\kappa_2',\pi' m'}^{--}(r,r') \sum_{\lambda_p\lambda_p'} \frac{\partial f_\pi^{\lambda_p}(r)}{\partial \rho_b^{\lambda_d}(r)} f_\pi^{\lambda_p'}(r') \sum_L \sum_{\lambda_y\lambda_y'}^{L\pm1} \mathcal{V}_L^{\lambda_y\lambda_y'}(r,r') \widehat{\mathcal{A}}_{\kappa_1'\kappa_2' m';\kappa_1\kappa_2 m}^{\lambda_p\lambda_p',L\lambda_y\lambda_y';--}. \tag{A49}$$

Besides, the contact term is introduced to compensate the zero-range term in $\mathcal{V}_L^{\lambda_y\lambda_y'}$ [see Eq. (A37)]. The Hartree contributions from the contact term are derived as zero, and the Fock contributions read as

$$E_\pi^\delta = -\frac{1}{2} \times \frac{1}{3} \sum_{ii'} (2-\delta_{\tau_i\tau_{i'}}) \int d\boldsymbol{r} d\boldsymbol{r}' \Big[\frac{f_\pi}{m_\pi} \bar{\psi}_{\nu\pi m} \gamma_5 \boldsymbol{\gamma} \psi_{\nu'\pi' m'} \Big]_{\boldsymbol{r}} \cdot \Big[\frac{f_\pi}{m_\pi} \bar{\psi}_{\nu'\pi' m'} \gamma_5 \boldsymbol{\gamma} \psi_{\nu\pi m} \Big]_{\boldsymbol{r}'} \delta(\boldsymbol{r}-\boldsymbol{r}'), \tag{A50}$$

where the δ function can be decomposed as

$$\delta(\boldsymbol{r}-\boldsymbol{r}') = \frac{\delta(r-r')}{r^2} \sum_{L=0}^{\infty} \sum_M (-1)^M Y_{LM}(\vartheta,\varphi) Y_{L-M}(\vartheta',\varphi'). \tag{A51}$$

To express the contact term compactly, we introduce the symbols $\mathscr{B}$ as

$$\widehat{\mathscr{B}}_{\kappa_1'\kappa_2' m';\kappa_1\kappa_2 m}^{\lambda_p\lambda_p';++} \equiv \frac{1}{2} \sum_{\lambda_d\lambda_d' L\sigma} \Big[\mathcal{Q}_{\kappa_1' m',\kappa_1 m}^{\lambda_d\mu\sigma} \mathcal{Q}_{\kappa_2' m',\kappa_2 m}^{\lambda_d'\mu\sigma} \Theta_{\lambda_d\lambda_p}^{L\mu} \Theta_{\lambda_d'\lambda_p'}^{L\mu} + \bar{\mathcal{Q}}_{\kappa_1' m',\kappa_1 m}^{\lambda_d\bar{\mu}\sigma} \bar{\mathcal{Q}}_{\kappa_2' m',\kappa_2 m}^{\lambda_d'\bar{\mu}\sigma} \Theta_{\lambda_d\lambda_p}^{L\bar{\mu}} \Theta_{\lambda_d'\lambda_p'}^{L\bar{\mu}} \Big], \tag{A52}$$

$$\widehat{\mathscr{B}}_{\kappa_1'\kappa_2' m';\kappa_1\kappa_2 m}^{\lambda_p\lambda_p';+-} \equiv \frac{1}{2} \sum_{\lambda_d\lambda_d' L\sigma} \Big[\mathcal{Q}_{\kappa_1' m',\kappa_1 m}^{\lambda_d\mu\sigma} \mathcal{Q}_{-\kappa_2' m',-\kappa_2 m}^{\lambda_d'\mu\sigma} \Theta_{\lambda_d\lambda_p}^{L\mu} \Theta_{\lambda_d'\lambda_p'}^{L\mu} + \bar{\mathcal{Q}}_{\kappa_1' m',\kappa_1 m}^{\lambda_d\bar{\mu}\sigma} \bar{\mathcal{Q}}_{-\kappa_2' m',-\kappa_2 m}^{\lambda_d'\bar{\mu}\sigma} \Theta_{\lambda_d\lambda_p}^{L\bar{\mu}} \Theta_{\lambda_d'\lambda_p'}^{L\bar{\mu}} \Big], \tag{A53}$$

$$\widehat{\mathscr{B}}_{\kappa_1'\kappa_2' m';\kappa_1\kappa_2 m}^{\lambda_p\lambda_p';-+} \equiv \frac{1}{2} \sum_{\lambda_d\lambda_d' L\sigma} \Big[\mathcal{Q}_{-\kappa_1' m',-\kappa_1 m}^{\lambda_d\mu\sigma} \mathcal{Q}_{\kappa_2' m',\kappa_2 m}^{\lambda_d'\mu\sigma} \Theta_{\lambda_d\lambda_p}^{L\mu} \Theta_{\lambda_d'\lambda_p'}^{L\mu} + \bar{\mathcal{Q}}_{-\kappa_1' m',-\kappa_1 m}^{\lambda_d\bar{\mu}\sigma} \bar{\mathcal{Q}}_{\kappa_2' m',\kappa_2 m}^{\lambda_d'\bar{\mu}\sigma} \Theta_{\lambda_d\lambda_p}^{L\bar{\mu}} \Theta_{\lambda_d'\lambda_p'}^{L\bar{\mu}} \Big], \tag{A54}$$

$$\widehat{\mathscr{B}}_{\kappa_1'\kappa_2' m';\kappa_1\kappa_2 m}^{\lambda_p\lambda_p';--} \equiv \frac{1}{2} \sum_{\lambda_d\lambda_d' L\sigma} \Big[\mathcal{Q}_{-\kappa_1' m',-\kappa_1 m}^{\lambda_d\mu\sigma} \mathcal{Q}_{-\kappa_2' m',-\kappa_2 m}^{\lambda_d'\mu\sigma} \Theta_{\lambda_d\lambda_p}^{L\mu} \Theta_{\lambda_d'\lambda_p'}^{L\mu} + \bar{\mathcal{Q}}_{-\kappa_1' m',-\kappa_1 m}^{\lambda_d\bar{\mu}\sigma} \bar{\mathcal{Q}}_{-\kappa_2' m',-\kappa_2 m}^{\lambda_d'\bar{\mu}\sigma} \Theta_{\lambda_d\lambda_p}^{L\bar{\mu}} \Theta_{\lambda_d'\lambda_p'}^{L\bar{\mu}} \Big]. \tag{A55}$$

Thus, the energy functional of the contact term can be expressed as

$$E_\pi^\delta = \frac{1}{2} \int dr \sum_i v_i^2 \sum_{\kappa_1\kappa_2} \begin{pmatrix} \mathcal{G}_{i\kappa_1}(r) & \mathcal{F}_{i\kappa_1}(r) \end{pmatrix} \begin{pmatrix} Y_{G,\pi m}^{\kappa_1\kappa_2,\pi\delta} & Y_{F,\pi m}^{\kappa_1\kappa_2,\pi\delta} \\ X_{G,\pi m}^{\kappa_1\kappa_2,\pi\delta} & X_{F,\pi m}^{\kappa_1\kappa_2,\pi\delta} \end{pmatrix}_{r,r} \begin{pmatrix} \mathcal{G}_{i\kappa_2}(r) \\ \mathcal{F}_{i\kappa_2}(r) \end{pmatrix}, \tag{A56}$$

where the self-energies read as

$$Y^{\kappa_1\kappa_2,\pi\delta}_{G,\pi m} = -\frac{1}{6\pi m_\pi^2 r^2}\sum_{\pi' m'}(2-\delta_{\tau\tau'})\sum_{\kappa_1'\kappa_2'}\mathcal{R}^{++}_{\kappa_1'\kappa_2',\pi' m'}(r,r)\sum_{\lambda_p\lambda_p'} f_\pi^{\lambda_p}(r) f_\pi^{\lambda_{p'}}(r)\widehat{\mathscr{B}}^{\lambda_p\lambda_p';++}_{\kappa_1'\kappa_2' m';\kappa_1\kappa_2 m}, \tag{A57}$$

$$Y^{\kappa_1\kappa_2,\pi\delta}_{F,\pi m} = -\frac{1}{6\pi m_\pi^2 r^2}\sum_{\pi' m'}(2-\delta_{\tau\tau'})\sum_{\kappa_1'\kappa_2'}\mathcal{R}^{+-}_{\kappa_1'\kappa_2',\pi' m'}(r,r)\sum_{\lambda_p\lambda_p'} f_\pi^{\lambda_p}(r) f_\pi^{\lambda_{p'}}(r)\widehat{\mathscr{B}}^{\lambda_p\lambda_p';+-}_{\kappa_1'\kappa_2' m';\kappa_1\kappa_2 m}, \tag{A58}$$

$$X^{\kappa_1\kappa_2,\pi\delta}_{G,\pi m} = -\frac{1}{6\pi m_\pi^2 r^2}\sum_{\pi' m'}(2-\delta_{\tau\tau'})\sum_{\kappa_1'\kappa_2'}\mathcal{R}^{-+}_{\kappa_1'\kappa_2',\pi' m'}(r,r)\sum_{\lambda_p\lambda_p'} f_\pi^{\lambda_p}(r) f_\pi^{\lambda_{p'}}(r)\widehat{\mathscr{B}}^{\lambda_p\lambda_p';-+}_{\kappa_1'\kappa_2' m';\kappa_1\kappa_2 m}, \tag{A59}$$

$$X^{\kappa_1\kappa_2,\pi\delta}_{F,\pi m} = -\frac{1}{6\pi m_\pi^2 r^2}\sum_{\pi' m'}(2-\delta_{\tau\tau'})\sum_{\kappa_1'\kappa_2'}\mathcal{R}^{--}_{\kappa_1'\kappa_2',\pi' m'}(r,r)\sum_{\lambda_p\lambda_p'} f_\pi^{\lambda_p}(r) f_\pi^{\lambda_{p'}}(r)\widehat{\mathscr{B}}^{\lambda_p\lambda_p';--}_{\kappa_1'\kappa_2' m';\kappa_1\kappa_2 m}. \tag{A60}$$

The rearrangement term in the self-energy can be derived as

$$\Sigma^{\delta,\lambda_d}_{R,\pi} = \sum_i v_i^2 \sum_{\kappa_1\kappa_2}\left(\begin{array}{cc}\mathcal{G}_{i\kappa_1}(r) & \mathcal{F}_{i\kappa_1}(r)\end{array}\right)\left(\begin{array}{cc}P^{\kappa_a\kappa_b,\pi\delta}_{G,\pi m,\lambda_d} & P^{\kappa_a\kappa_b,\pi\delta}_{F,\pi m,\lambda_d}\\ Q^{\kappa_a\kappa_b,\pi\delta}_{G,\pi m,\lambda_d} & Q^{\kappa_a\kappa_b,\pi\delta}_{F,\pi m,\lambda_d}\end{array}\right)_{r,r}\left(\begin{array}{c}\mathcal{G}_{i\kappa_2}(r)\\ \mathcal{F}_{i\kappa_2}(r)\end{array}\right), \tag{A61}$$

with the P and Q terms as

$$P^{\kappa_1\kappa_2,\pi\delta}_{G,\pi m,\lambda_d} = -\frac{1}{6\pi m_\pi^2 r^2}\sum_{\pi' m'}(2-\delta_{\tau\tau'})\sum_{\kappa_1'\kappa_2'}\mathcal{R}^{++}_{\kappa_1'\kappa_2',\pi' m'}(r,r)\sum_{\lambda_p\lambda_p'}\frac{\partial f_\pi^{\lambda_p}(r)}{\partial\rho_b^{\lambda_d}(r)} f_\pi^{\lambda_{p'}}(r)\widehat{\mathscr{B}}^{\lambda_p\lambda_p';++}_{\kappa_1'\kappa_2' m';\kappa_1\kappa_2 m}, \tag{A62}$$

$$P^{\kappa_1\kappa_2,\pi\delta}_{F,\pi m,\lambda_d} = -\frac{1}{6\pi m_\pi^2 r^2}\sum_{\pi' m'}(2-\delta_{\tau\tau'})\sum_{\kappa_1'\kappa_2'}\mathcal{R}^{+-}_{\kappa_1'\kappa_2',\pi' m'}(r,r)\sum_{\lambda_p\lambda_p'}\frac{\partial f_\pi^{\lambda_p}(r)}{\partial\rho_b^{\lambda_d}(r)} f_\pi^{\lambda_{p'}}(r)\widehat{\mathscr{B}}^{\lambda_p\lambda_p';+-}_{\kappa_1'\kappa_2' m';\kappa_1\kappa_2 m}, \tag{A63}$$

$$Q^{\kappa_1\kappa_2,\pi\delta}_{G,\pi m,\lambda_d} = -\frac{1}{6\pi m_\pi^2 r^2}\sum_{\pi' m'}(2-\delta_{\tau\tau'})\sum_{\kappa_1'\kappa_2'}\mathcal{R}^{-+}_{\kappa_1'\kappa_2',\pi' m'}(r,r)\sum_{\lambda_p\lambda_p'}\frac{\partial f_\pi^{\lambda_p}(r)}{\partial\rho_b^{\lambda_d}(r)} f_\pi^{\lambda_{p'}}(r)\widehat{\mathscr{B}}^{\lambda_p\lambda_p';-+}_{\kappa_1'\kappa_2' m';\kappa_1\kappa_2 m}, \tag{A64}$$

$$Q^{\kappa_1\kappa_2,\pi\delta}_{F,\pi m,\lambda_d} = -\frac{1}{6\pi m_\pi^2 r^2}\sum_{\pi' m'}(2-\delta_{\tau\tau'})\sum_{\kappa_1'\kappa_2'}\mathcal{R}^{--}_{\kappa_1'\kappa_2',\pi' m'}(r,r)\sum_{\lambda_p\lambda_p'}\frac{\partial f_\pi^{\lambda_p}(r)}{\partial\rho_b^{\lambda_d}(r)} f_\pi^{\lambda_{p'}}(r)\widehat{\mathscr{B}}^{\lambda_p\lambda_p';--}_{\kappa_1'\kappa_2' m';\kappa_1\kappa_2 m}. \tag{A65}$$